Metallic Magnetic Calorimeters for high precision X-ray spectroscopy

Loredana Gastaldo
Kirchhoff Institute for Physics
Heidelberg University
K

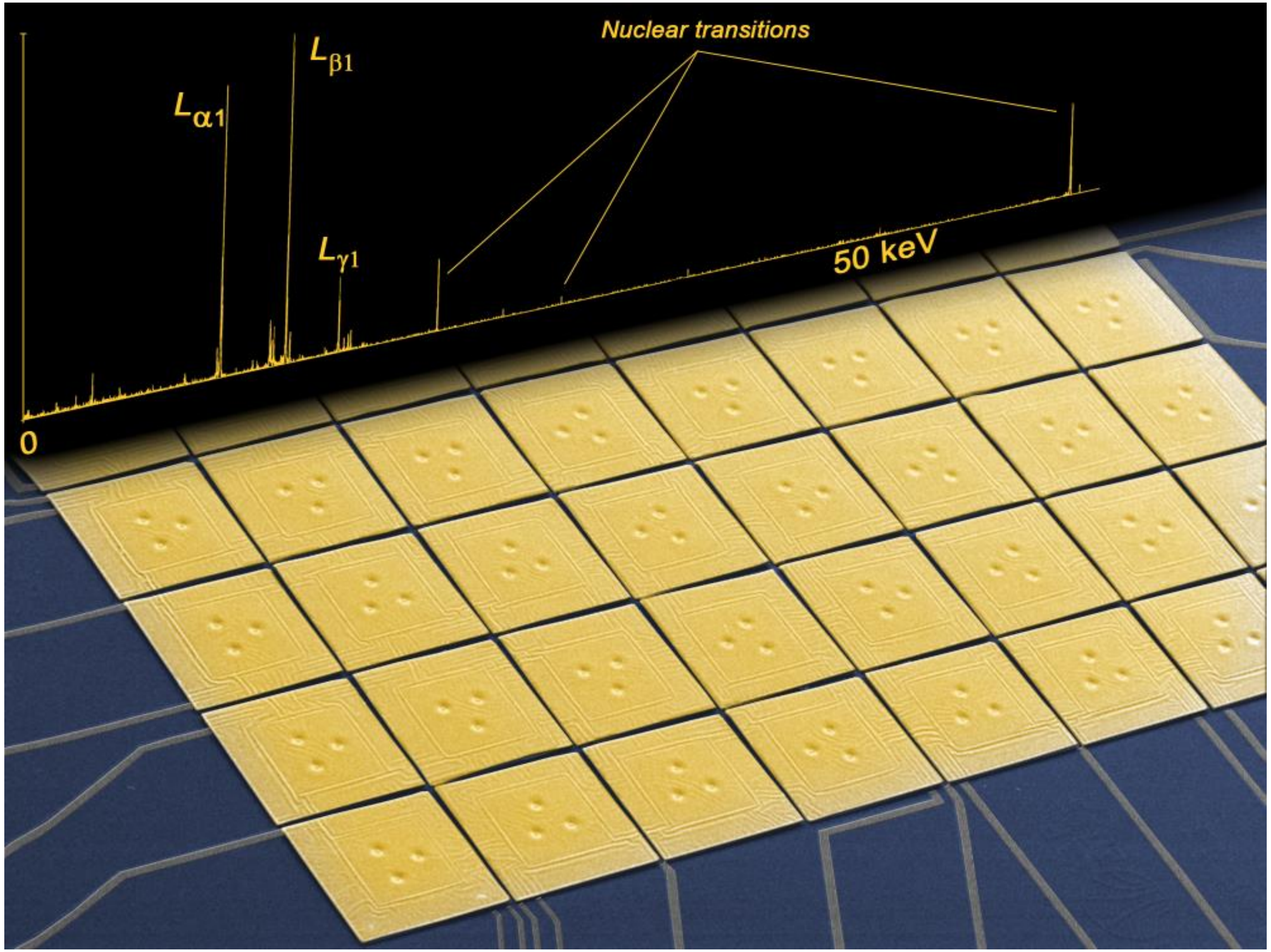

UNIVERSITÄT HEIDELBERG ZUKUNFT SEIT 1386

Outline

- Metallic magnetic calorimeters
  - Thermodynamical properties
  - Fabrication
  - Readout
- MMC applications and performance
  - $^{241}Am/^{233}U$
  - Highly charged heavy ions
  - Muonic Atoms
  - Electron capture sources
- Conclusions

Low Temperature Calorimeters

Near equilibrium detectors

Energy deposition induces increase of temperature

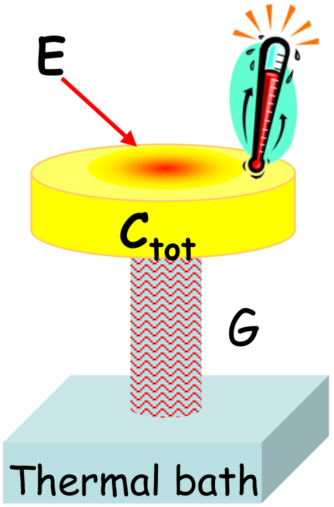

$$\Delta T \cong \frac{E}{C_{tot}}$$

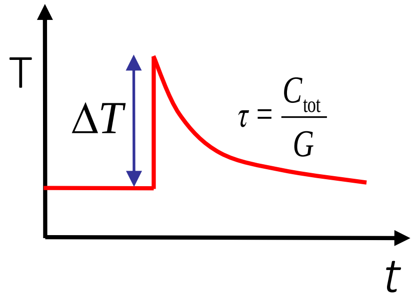

- Very small volume
- Working temperature below 100 mK

  small specific heat

  small thermal noise
- **Very sensitive temperature sensors**

Low Temperature Calorimeters

Near equilibrium detectors

Energy deposition induces increase of temperature

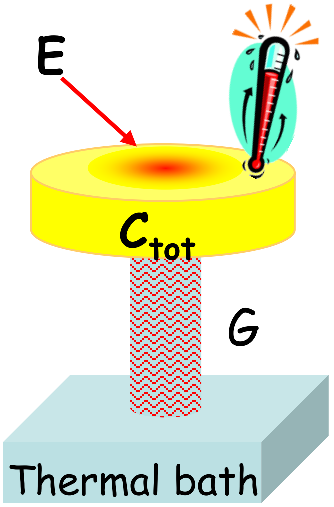

$$\Delta T \cong \frac{E}{C_{tot}}$$

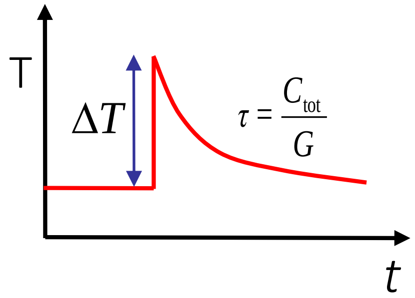

- Very small volume
- Working temperature below 100 mK
  - small specific heat
  - small thermal noise
- **Very sensitive temperature sensors**

Resistance of highly doped semiconductors

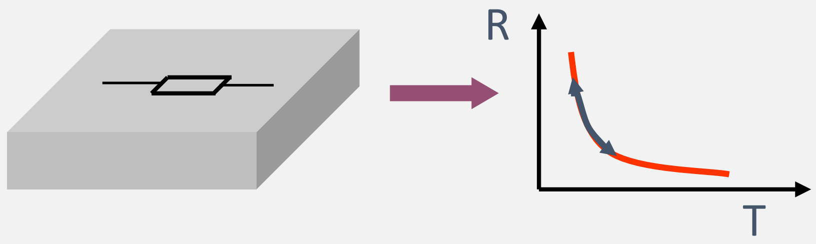

Resistance at superconducting transition,TES

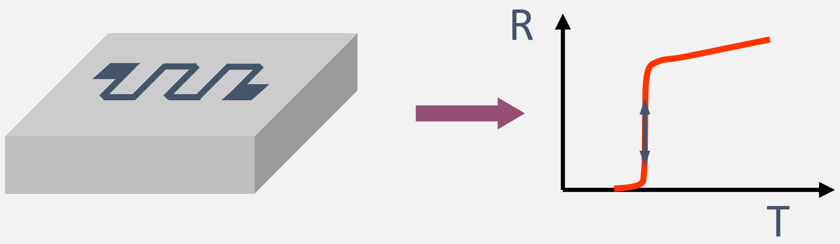

Magnetization of paramagnetic material, MMC

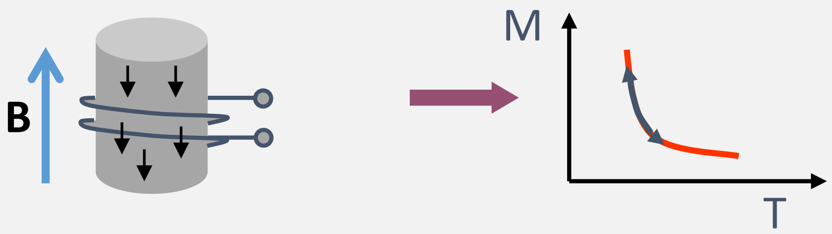

Metallic Magnetic Calorimeters

A.Fleischmann, C. Enss and G. M. Seidel,
Topics in Applied Physics **99** (2005) 63

A.Fleischmann et al.,
AIP Conf. Proc. **1185** (2009) 571

M. Herbst et al.,
J Low Temp Phys **202** (2021) 106

Paramagnetic temperature sensor

Dilute alloy Au:Er or Ag:Er (Er concentration: a few hundred ppm)

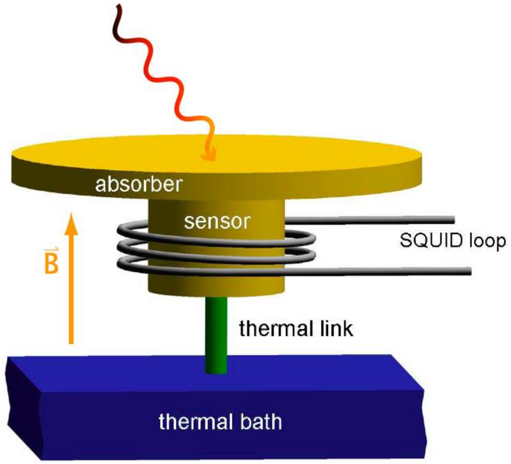

$$\Delta T \cong \frac{E}{C_{\text{tot}}}$$

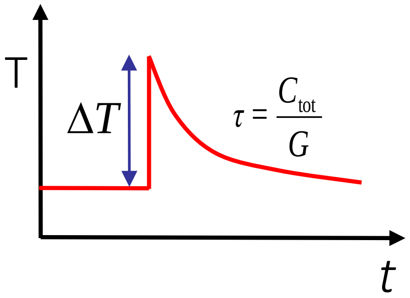

Metallic Magnetic Calorimeters

A.Fleischmann, C. Enss and G. M. Seidel, Topics in Applied Physics **99** (2005) 63

A.Fleischmann et al., *AIP Conf. Proc.* **1185** (2009) 571

M. Herbst et al., J Low Temp Phys **202** (2021) 106

Paramagnetic temperature sensor

Dilute alloy Au:Er or Ag:Er (Er concentration: a few hundred ppm)

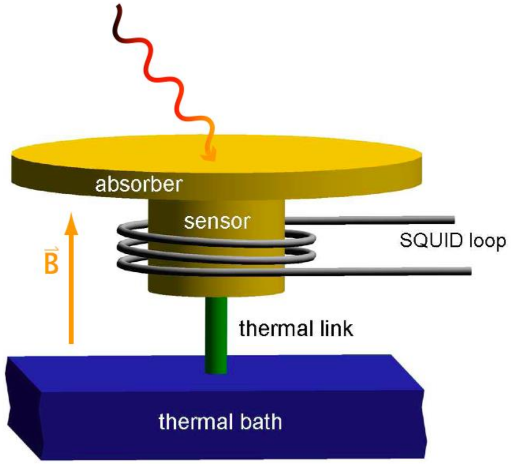

$$\Delta T \cong \frac{E}{C_{\mathrm{tot}}} \quad \xrightarrow{\text{MMC}} \quad \Delta\Phi_S \propto \frac{\partial M}{\partial T}\Delta T \rightarrow \Delta\Phi_S \propto \frac{\partial M}{\partial T}\frac{E}{C_{\mathrm{tot}}}$$

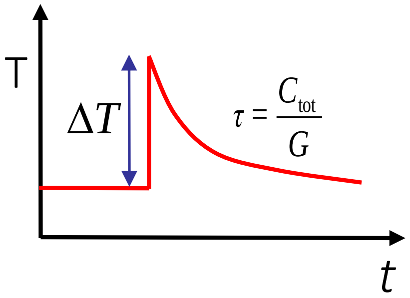

Metallic Magnetic Calorimeters

A.Fleischmann, C. Enss and G. M. Seidel, Topics in Applied Physics **99** (2005) 63

A.Fleischmann et al., *AIP Conf. Proc.* **1185** (2009) 571

M. Herbst et al., J Low Temp Phys **202** (2021) 106

Paramagnetic temperature sensor

Dilute alloy Au:Er or Ag:Er   (Er concentration: a few hundred ppm)

$$\Delta T \cong \frac{E}{C_{tot}} \xrightarrow{\text{MMC}} \Delta\Phi_S \propto \frac{\partial M}{\partial T}\Delta T \rightarrow \Delta\Phi_S \propto \frac{\partial M}{\partial T}\frac{E}{C_{tot}}$$

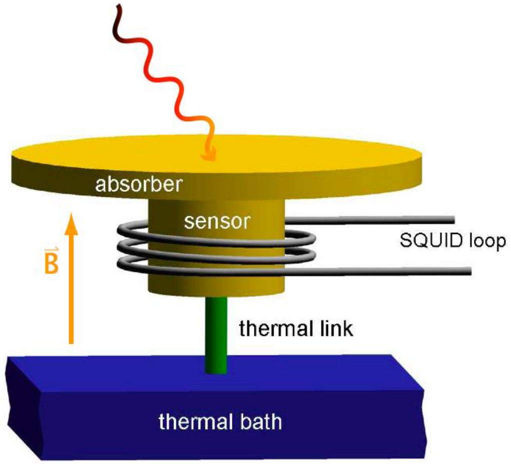

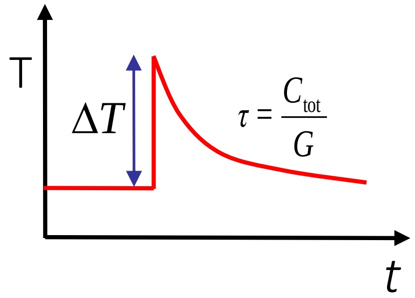

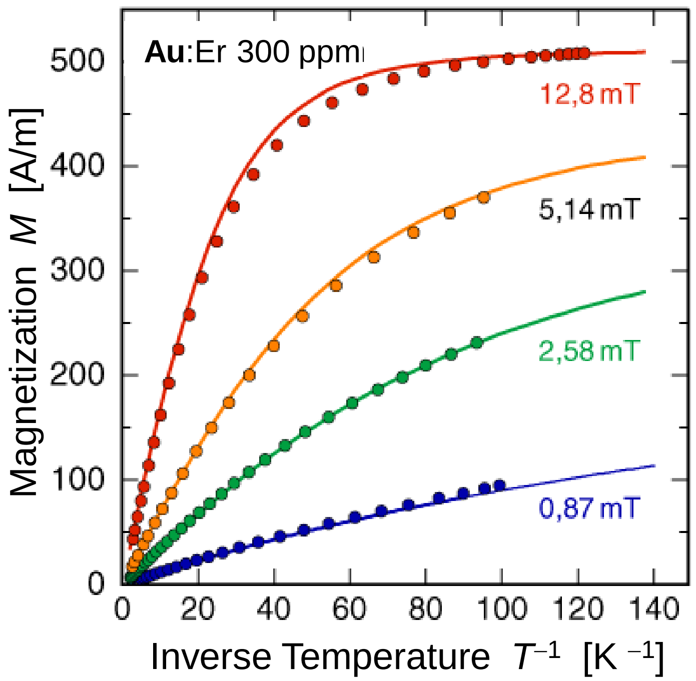

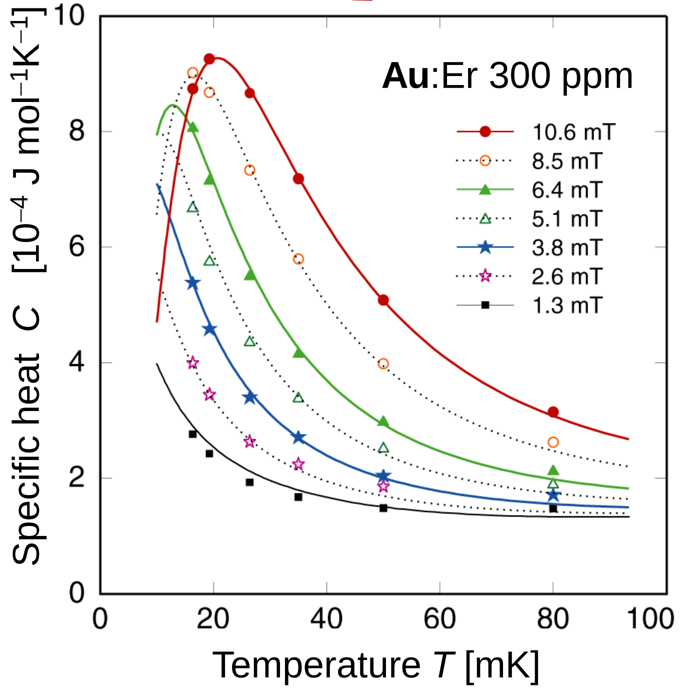

Very good agreement between data and theoretical expectation for interacting spin system

Performance

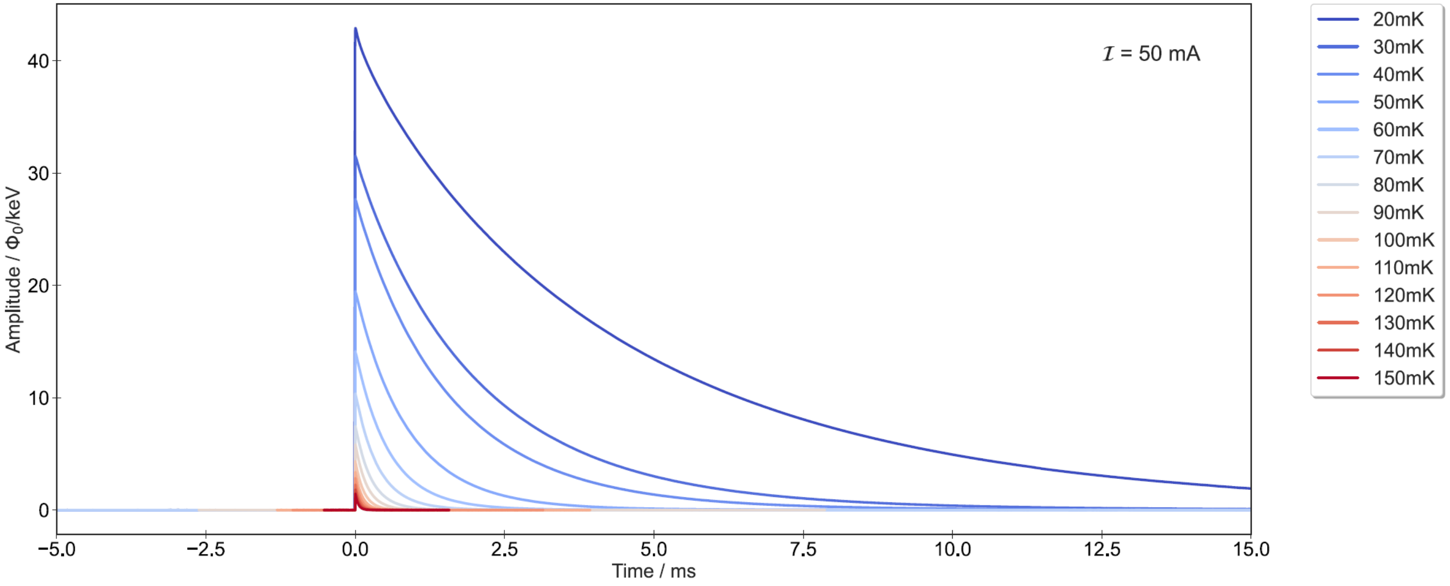

Operation over a large temperature range

→ operation of large arrays

Large dynamic range

→ no saturation of the signal

Design defined decay constant

→ thermal link optimized for detector heat capacity at operating temperature

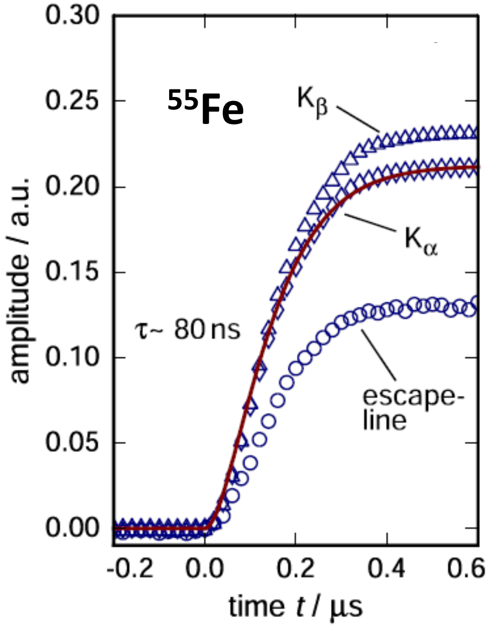

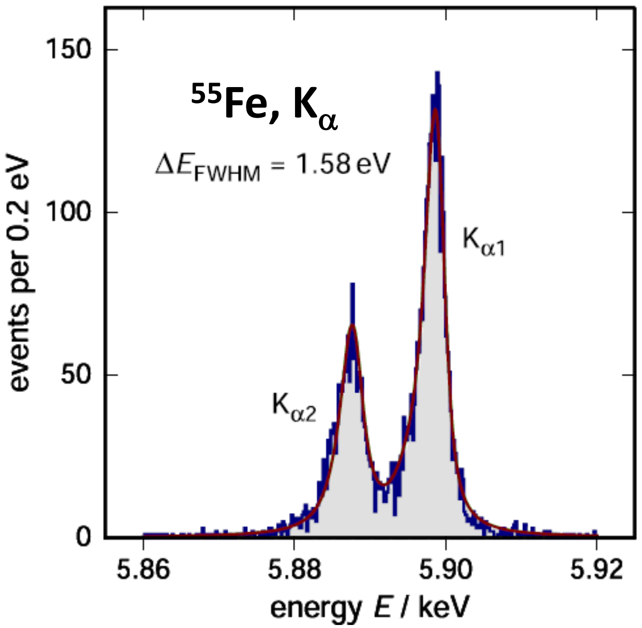

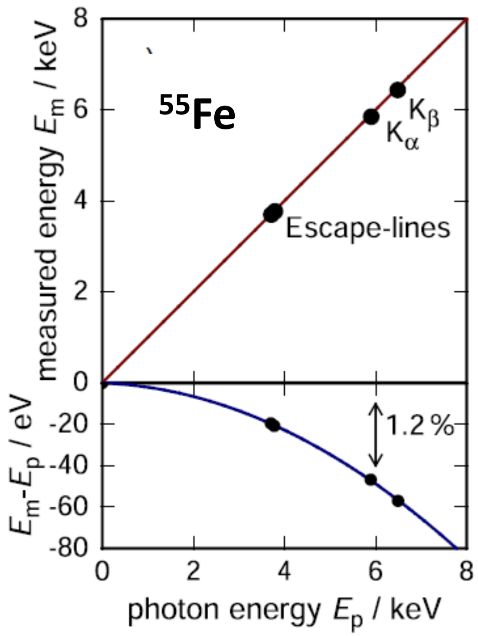

Fast risetime

→ Reduction un-resolved pile-up

Extremely good energy resolution

→ identification of small structures

Excellent linearity

→ precise definition of the energy scale

Detector geometries

- planar paramagnetic sensor
- superconducting coil
- transformed coupled to a dc SQUID

Well established:
- superconducting meander shaped pickup loop
- planar sensor on top of meander-shaped coil
- gradiometric design

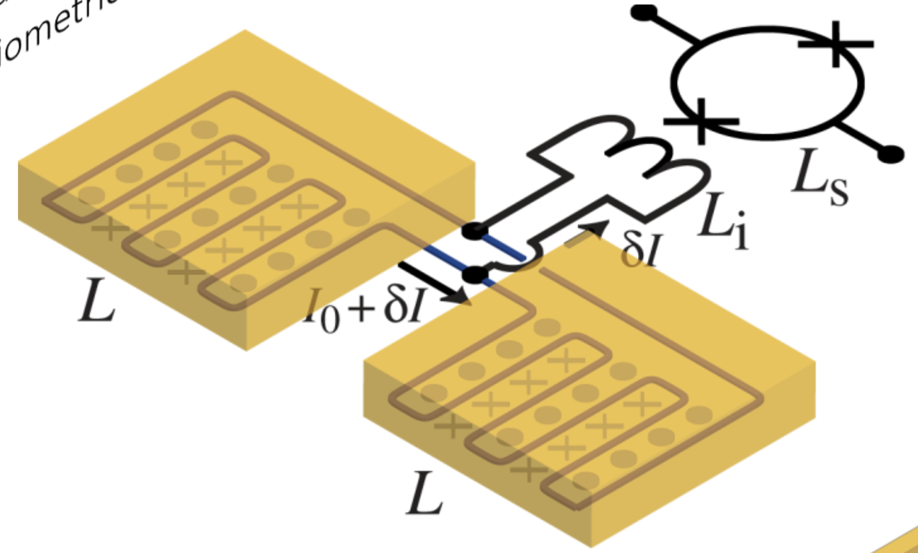

Sandwich geometry:
- planar sensor sandwiched between stripline
- best magnetic flux coupling

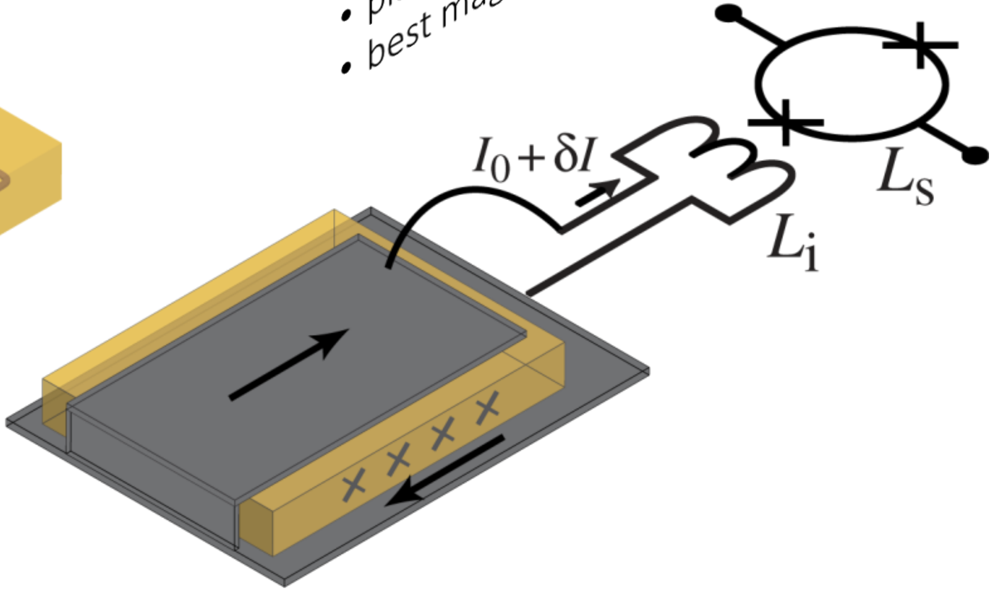

Microcalorimeter arrays for X-rays spectroscopy - maXs

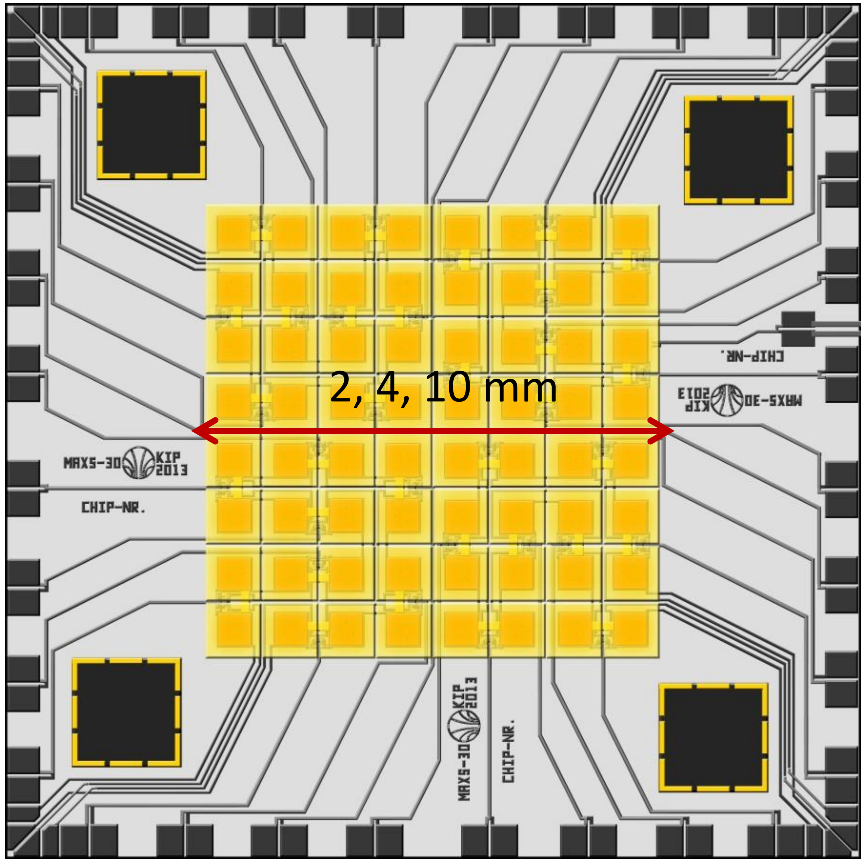

maXs-20/30/100:

- 8×8 pixels for photons up to 20/30/100 keV
- with ΔE_{FWHM} = 2/5/30 eV
- 32 two-stage dc-SQUIDs

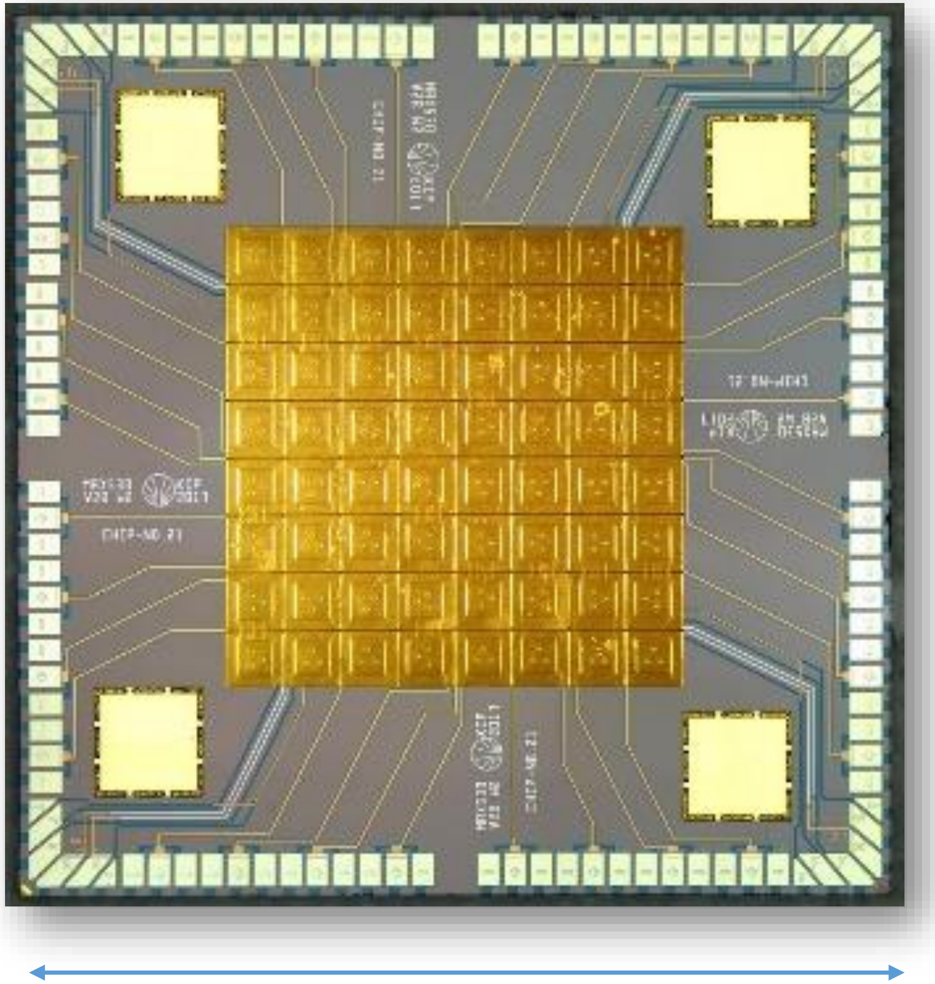

maXs-30

Absorber size: 500 × 500 × 30 μm^3

MMC fabrication

40 m^2 Cleanroom class 100
at Kirchhoff Institute for Physics

Wet bench
Chemistry bench
Maskless aligner
UHV sputtering system
Dry etching system

- Flexibility in design and fabrication
- Reliable processes for thin films
- Production of MMC array and superconducting electronics

MMC readout

Two-stage dc-SQUID readout with flux-locked loop

low noise

small power dissipation on detector SQUID chip (voltage bias 1st stage)

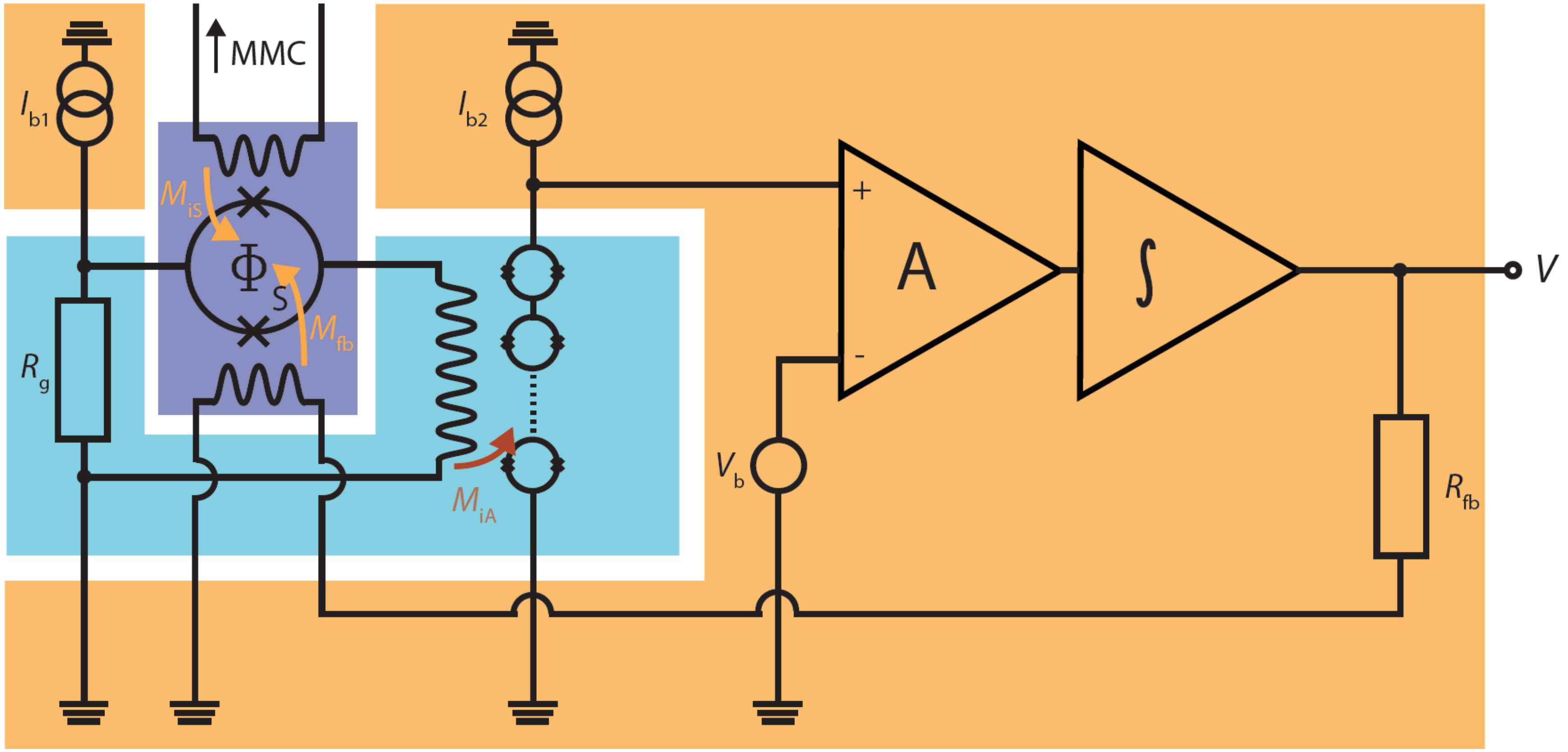

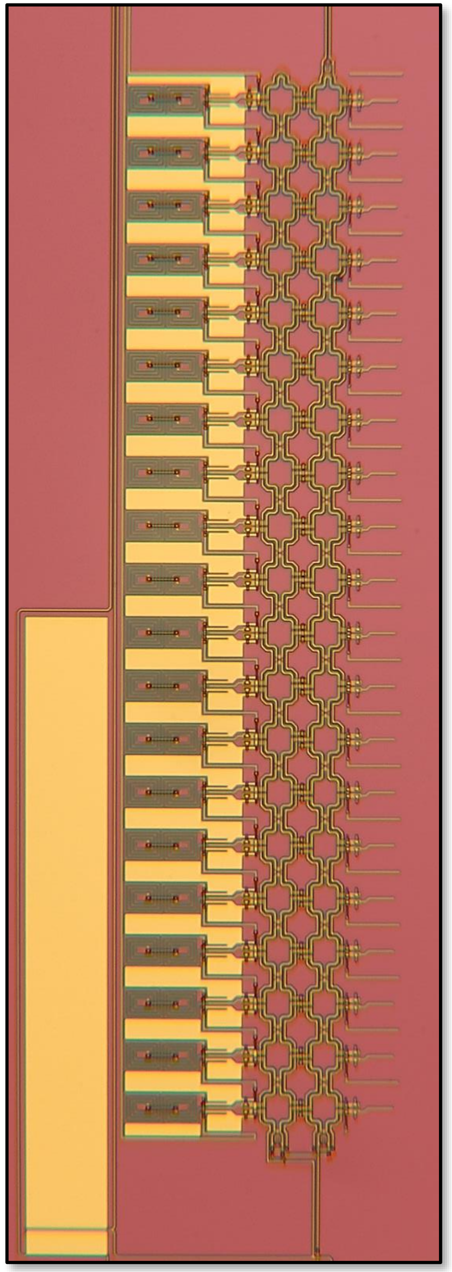

In house produced SQUID array

maXs-30 set-up

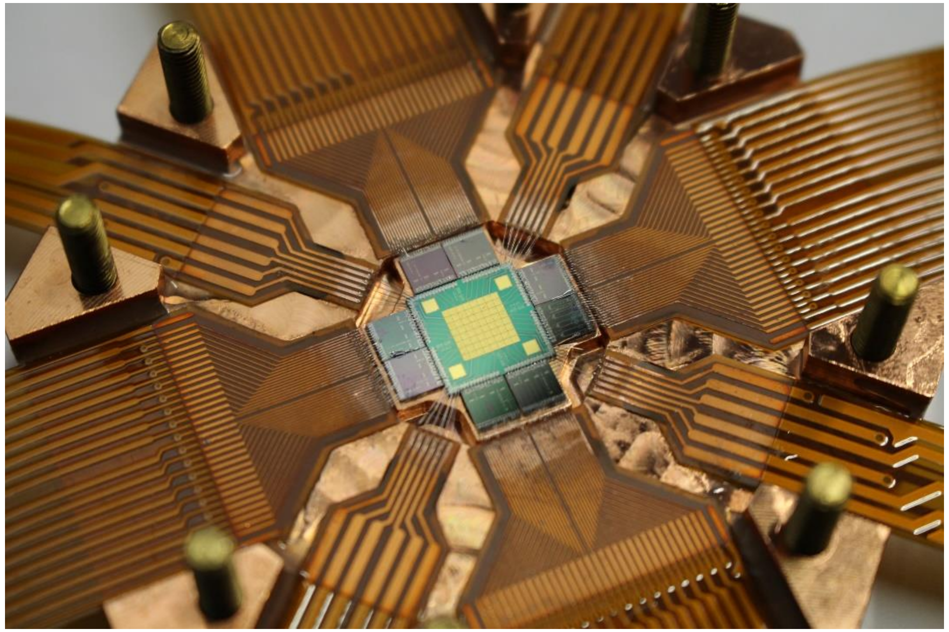

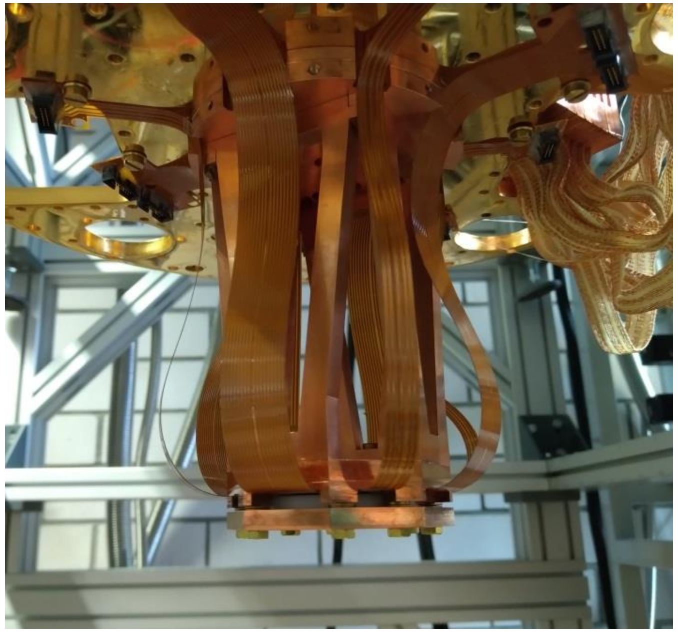

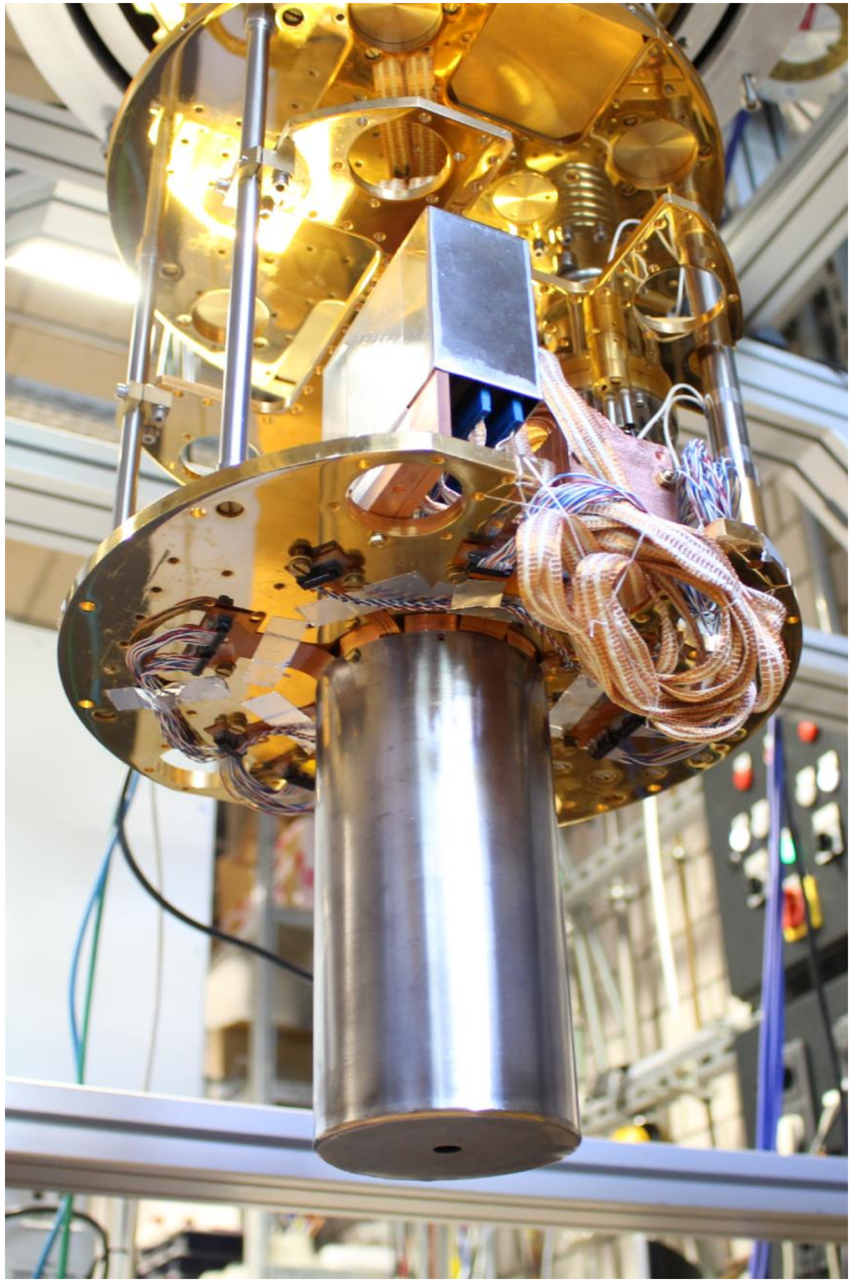

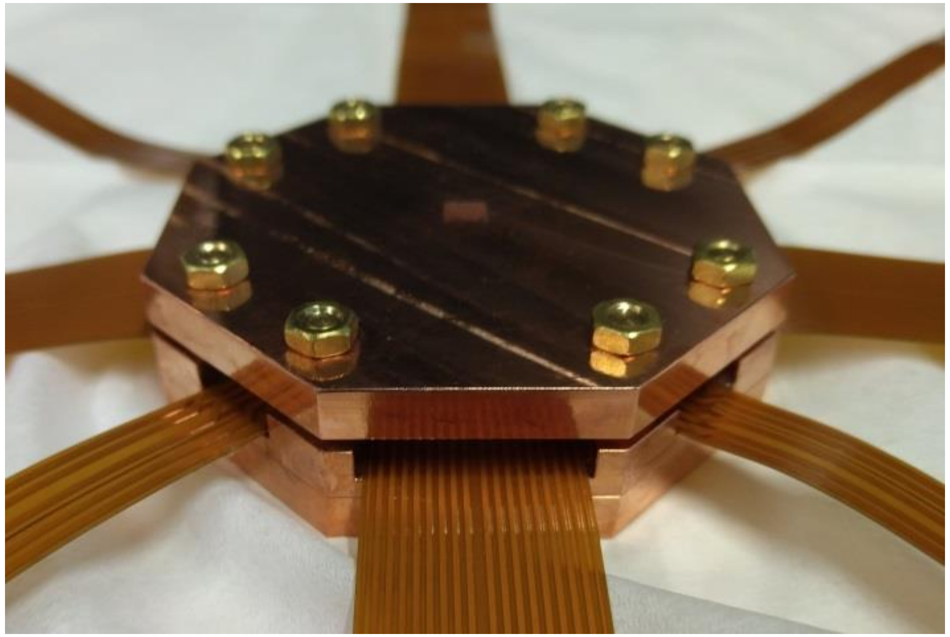

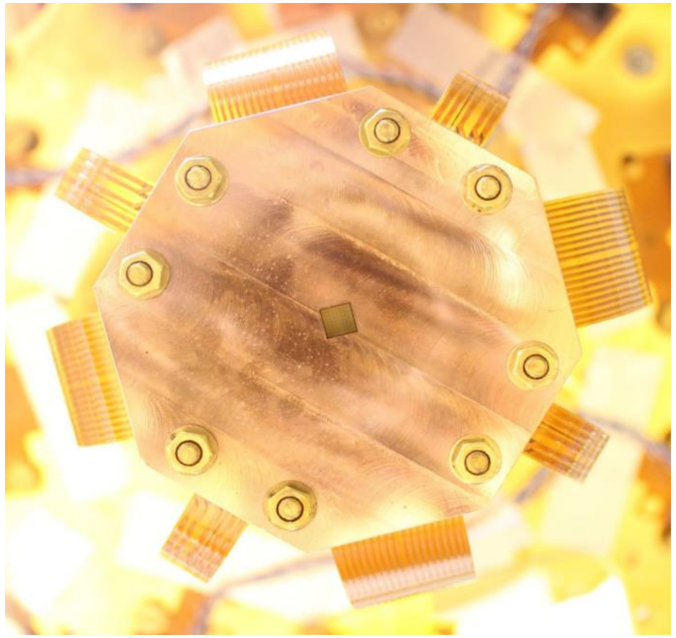

Applications and Performance

maXs-30 set-up - ^{55}Fe calibration

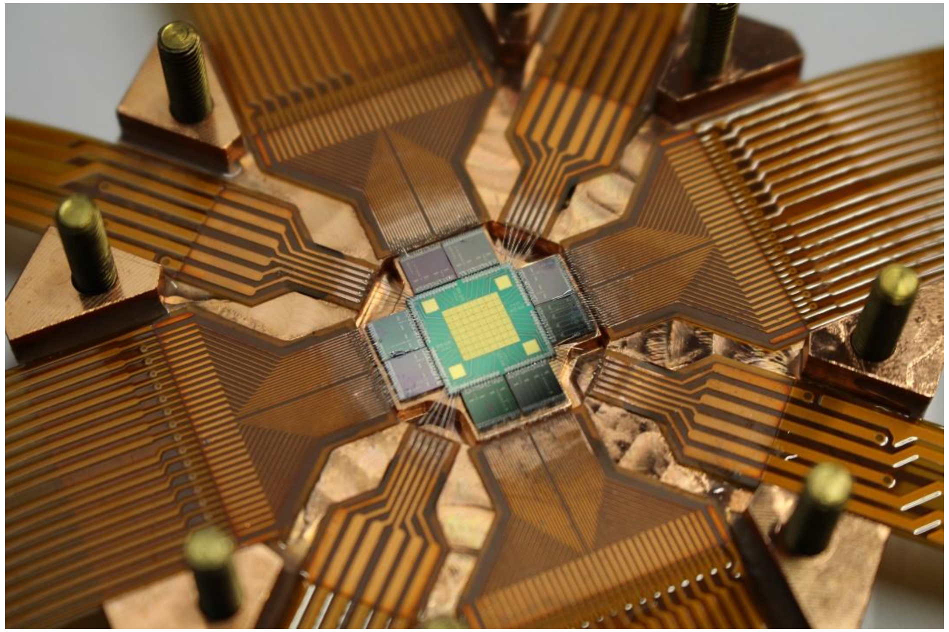

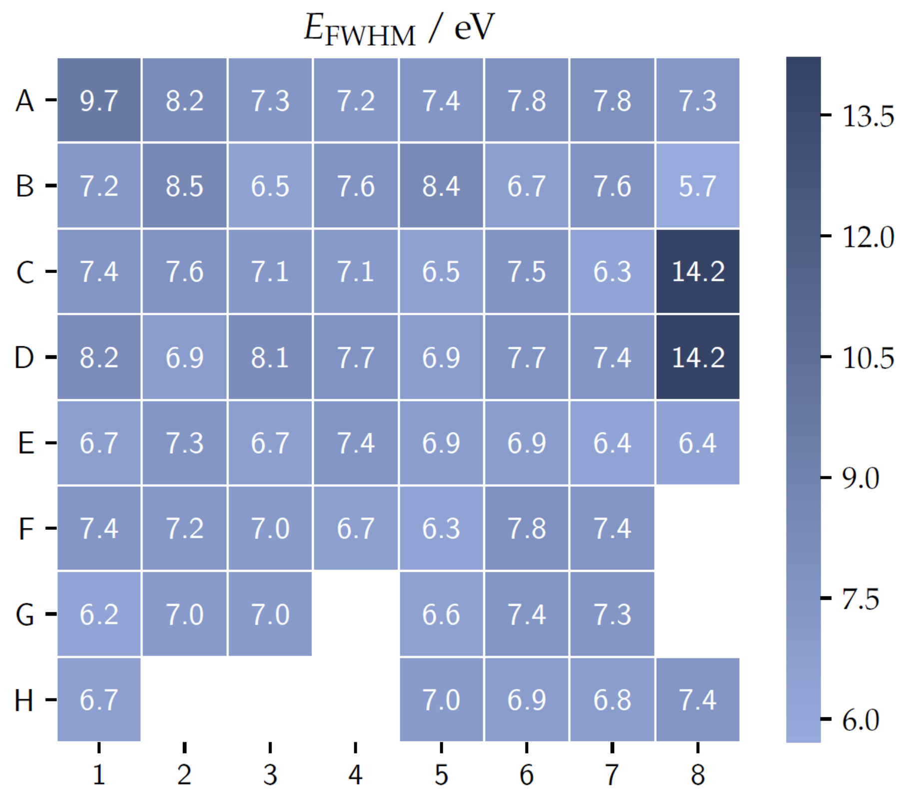

^{55}Fe calibration source

Stopping power @10 keV ~100%

- Homogeneous performance over the array
- Stable operation over 1 month

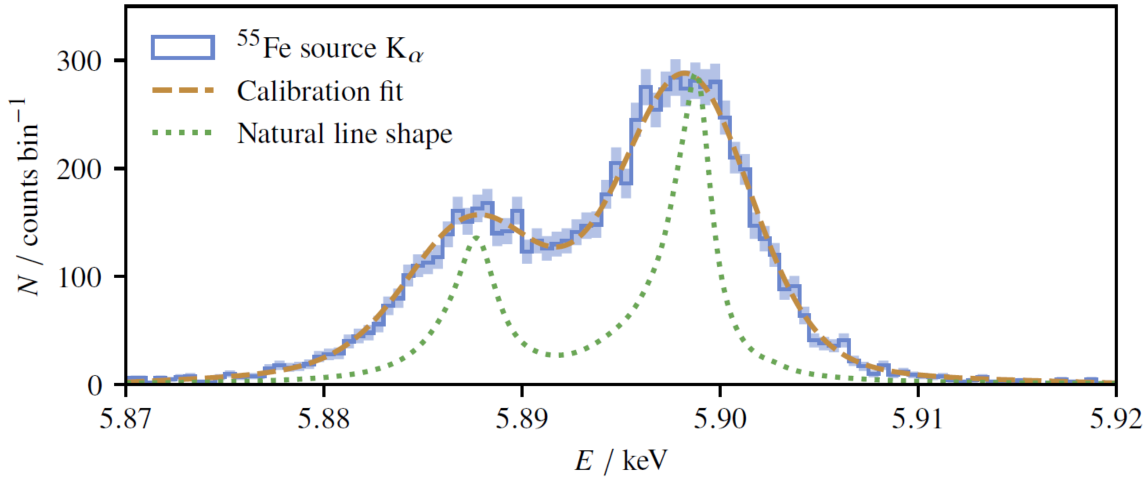

D. Unger et al., *JINST* **16** (2021) P06006, arXiv:2010.15348 [physics.ins-det]

maXs-30 set-up - ^{241}Am + ^{233}U external sources

Co-added 20 channels, several weeks

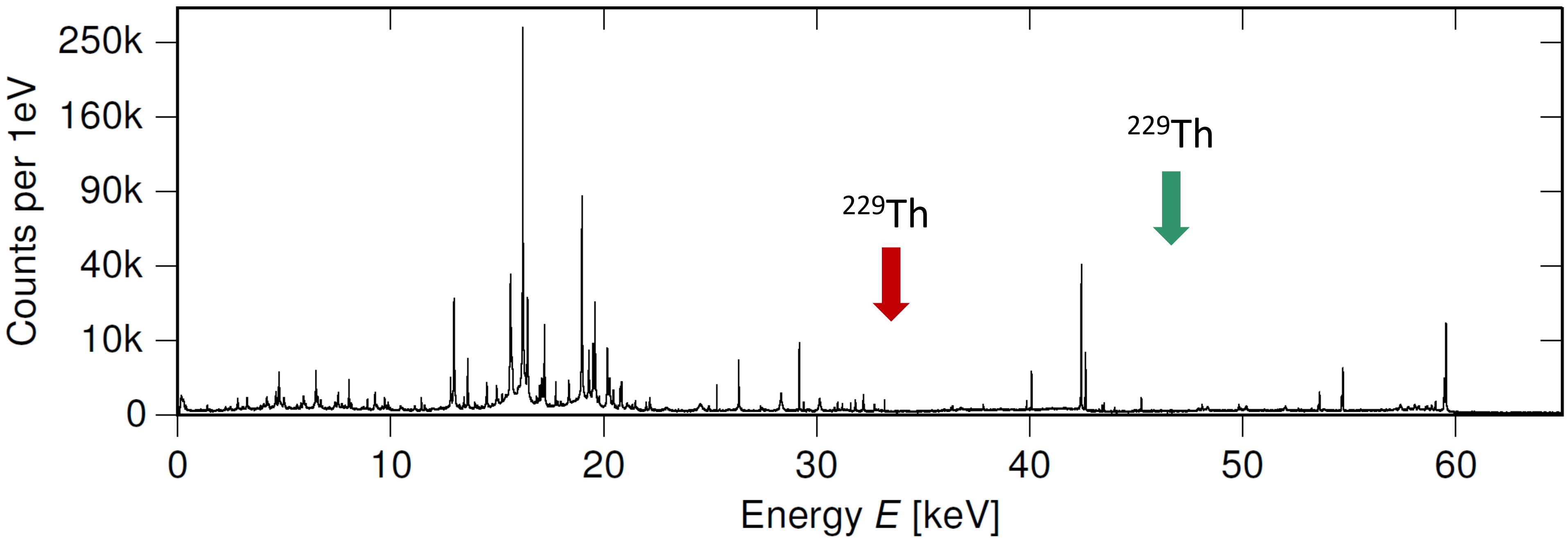

Isomer energy: ΔE_{iso} = 8.10 eV ± 0.17 eV

in fair agreement with previous result 7.8 eV ± 0.5eV

T. Sikorsky et al., *Phys. Rev. Lett.* **125** (2020) 142503

maXs-30 set-up - ^{241}Am + ^{233}U external sources

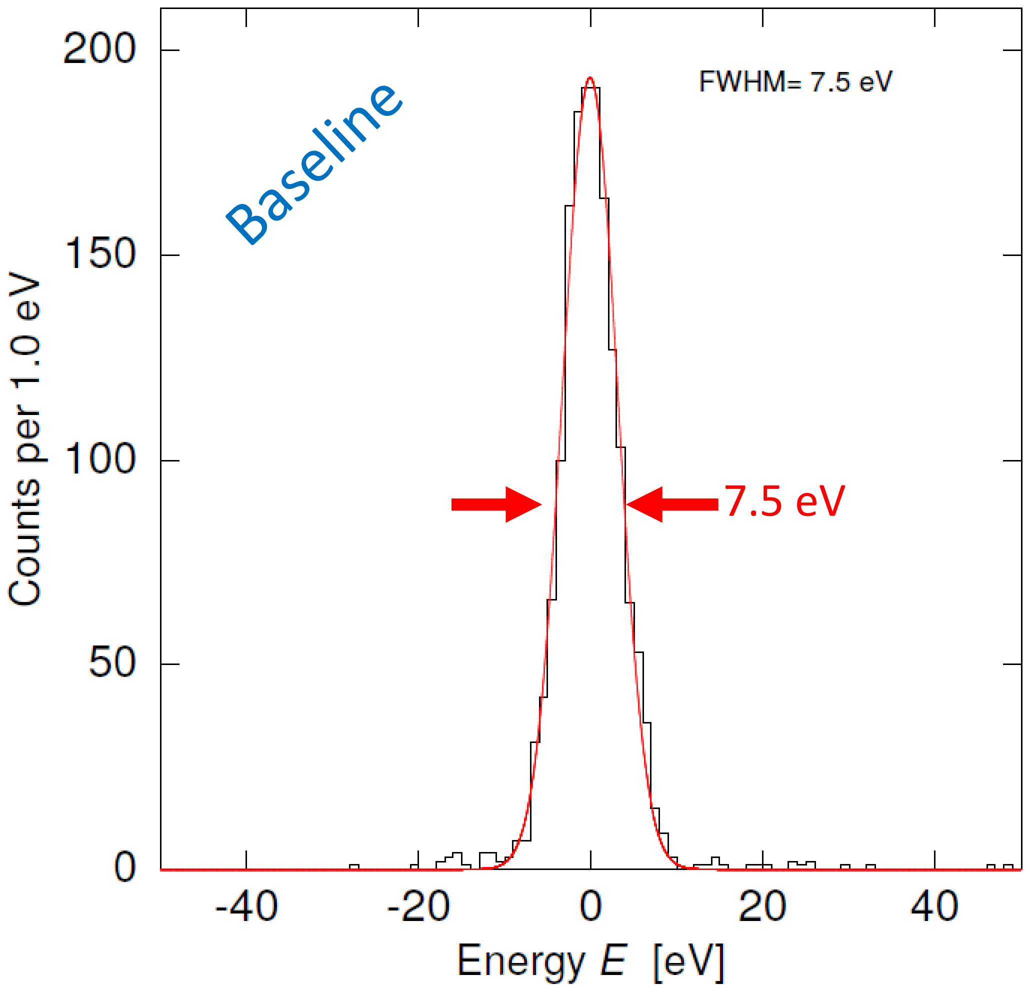

Very close to design value

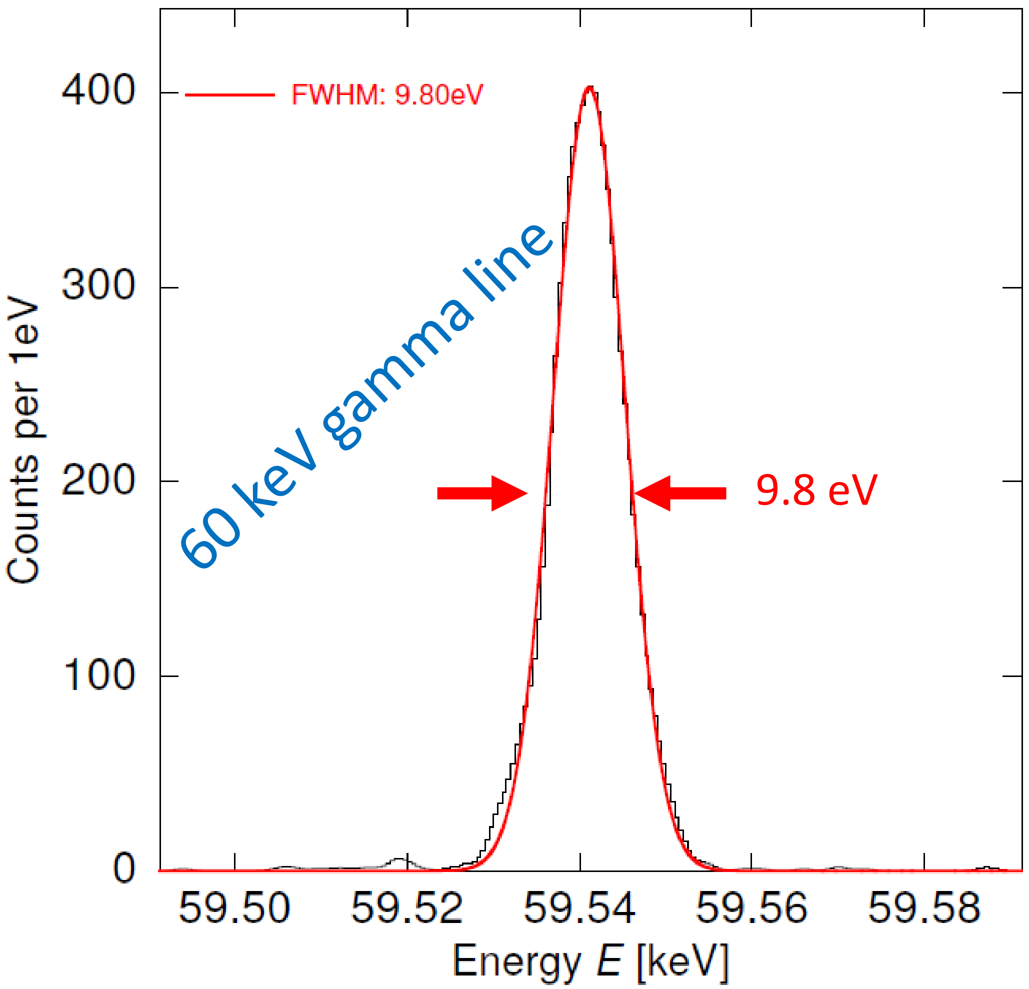

Energy resolution ΔE_{FWHM} = 9.8 eV @ 59 keV

World record resolving power: 6000

T. Sikorsky et al., *Phys. Rev. Lett.* **125** (2020) 142503

maXs-30 set-up - ^{241}Am + ^{233}U external sources

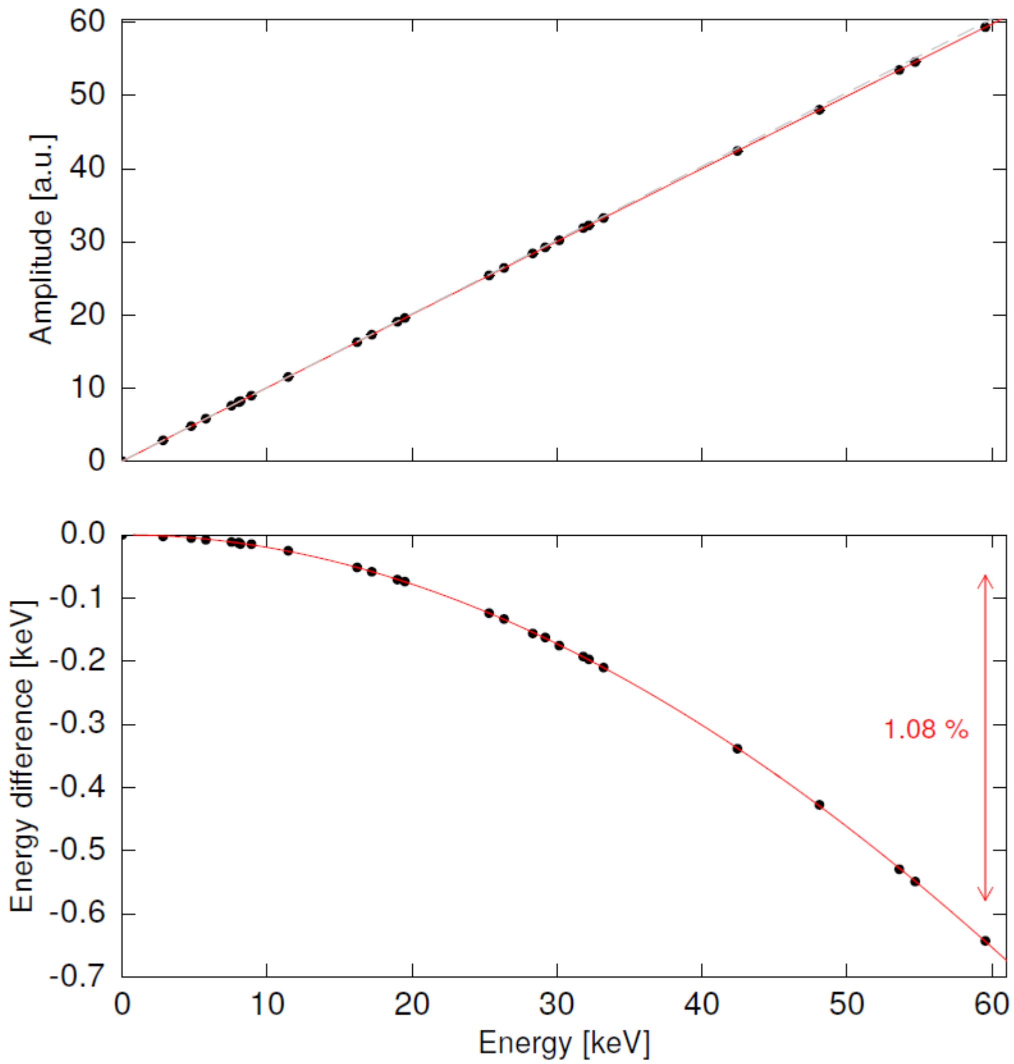

Energy calibration

- Polynomial function 2nd to 4th order
- Stable over long measuring time

non-linearity as expected from thermodynamics!

T. Sikorsky et al., *Phys. Rev. Lett.* **125** (2020) 142503

maXs-30 set-up - ^{241}Am + ^{233}U external sources

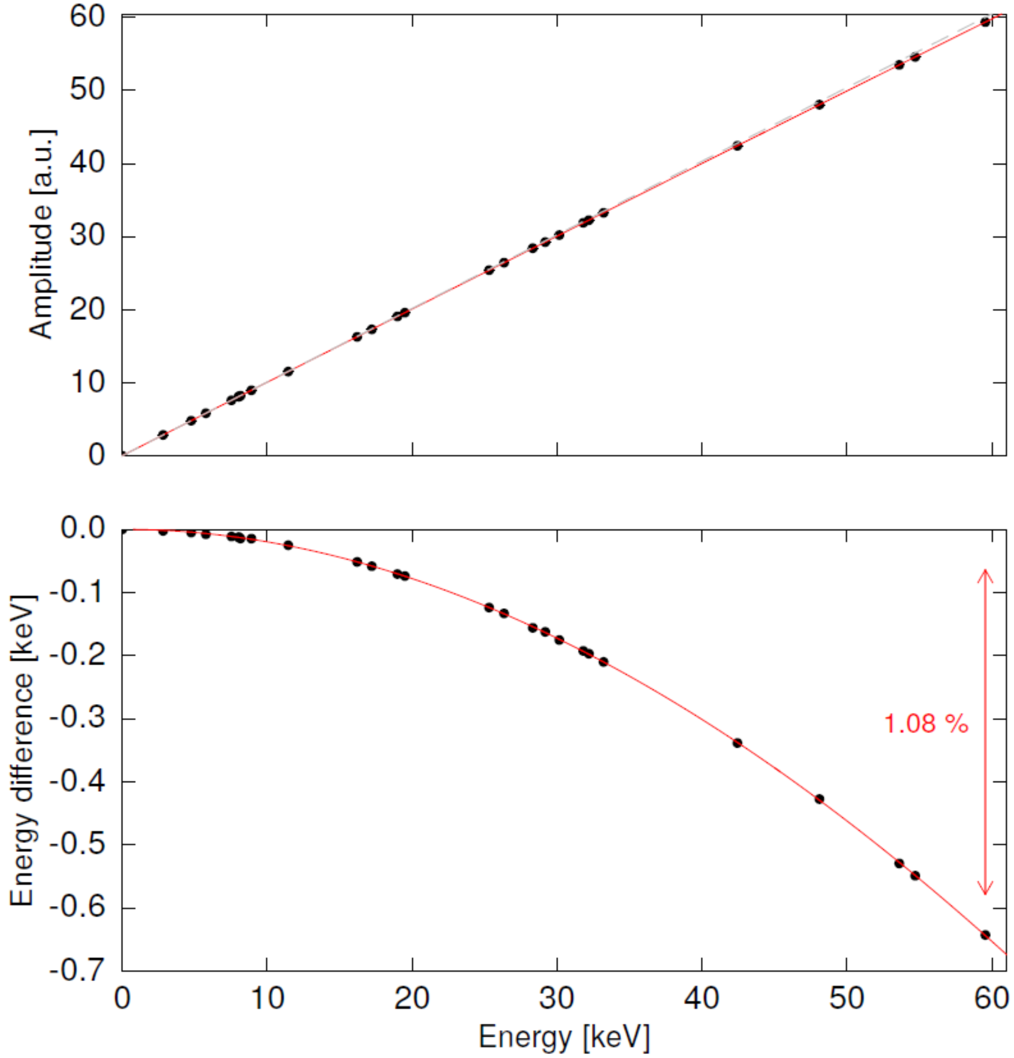

Energy calibration

- Polynomial function 2nd to 4th order
- Stable over long measuring time

Most lines from literature have too large uncertainty!

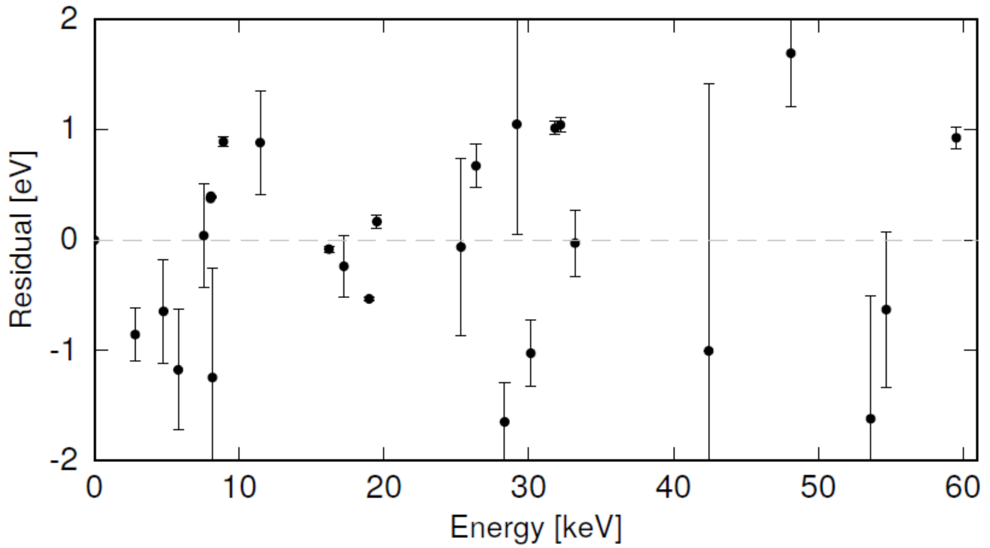

non-linearity as expected from thermodynamics!

T. Sikorsky et al., *Phys. Rev. Lett.* **125** (2020) 142503

maXs-30 set-up - ^{241}Am + ^{233}U external sources

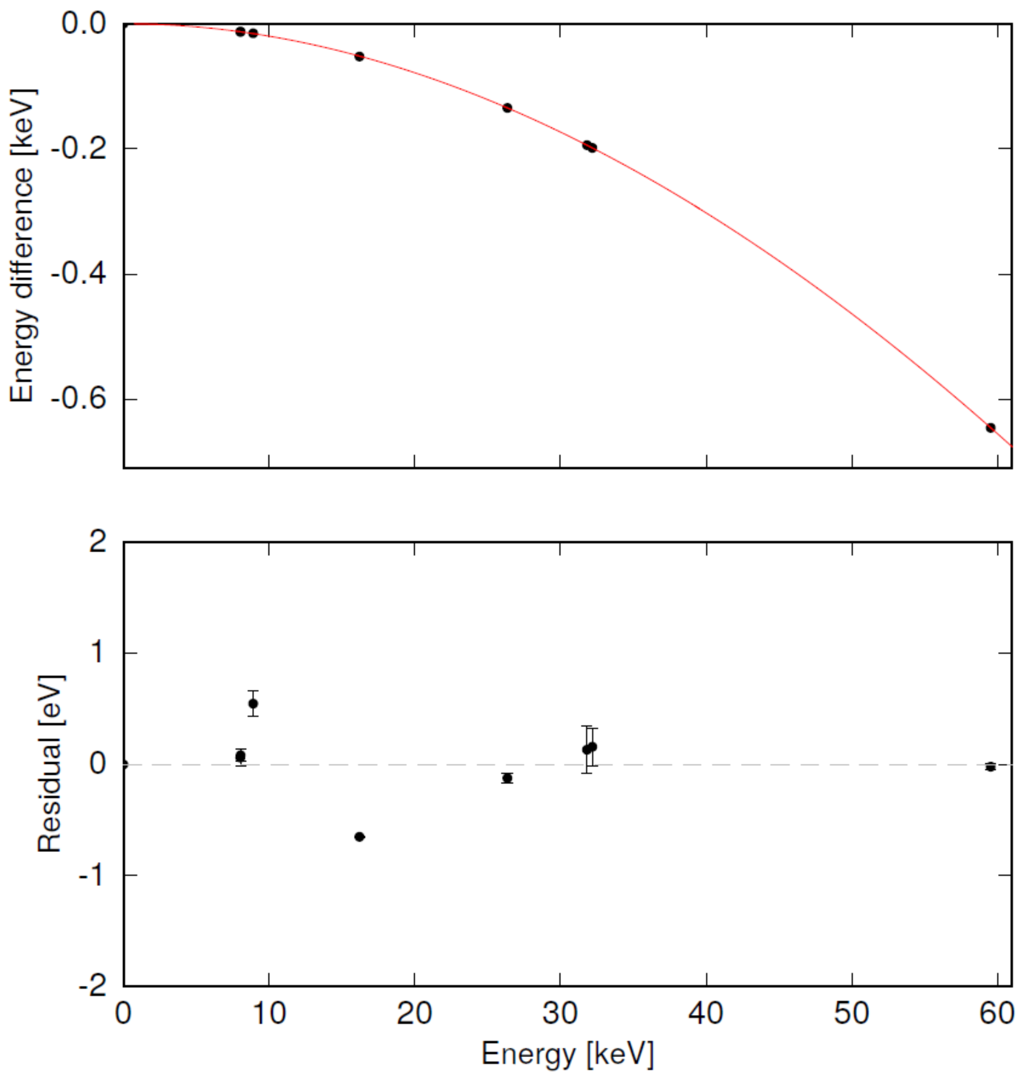

Energy calibration

- Polynomial function 2nd to 4th order
- Stable over long measuring time

Sub-eV agreement for carefully selected calibration lines.

non-linearity as expected from thermodynamics!

T. Sikorsky et al., *Phys. Rev. Lett.* **125** (2020) 142503

maXs-30 set-up - ^{241}Am + ^{233}U external sources

i) from transitions within lowest 5 states

B.R. Beck et al, PRL 98, 142501 (2007)

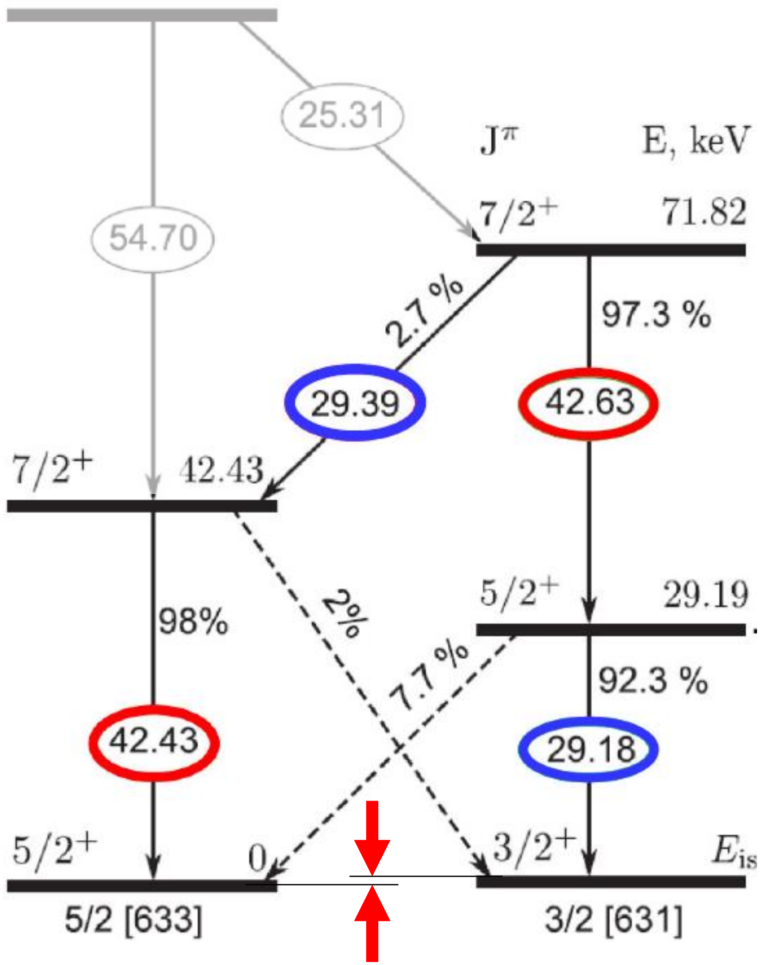

$$E_{iso} = E_{29.39\,keV} - E_{29.18\,keV} - (E_{42.63\,keV} - E_{42.43\,keV})$$
$$= \Delta E_{29\,keV} - \Delta E_{42\,keV}$$

ii) resolving the 29.2keV doublet

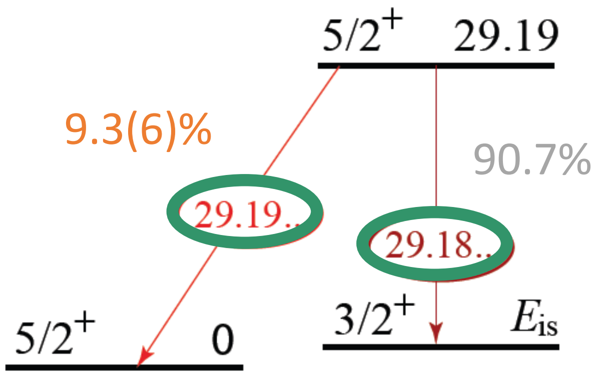

T. Sikorsky et al., *Phys. Rev. Lett.* **125** (2020) 142503

maXs-30 set-up - ^{241}Am + ^{233}U external sources

i) from transitions within lowest 5 states

ii) resolving the 29.2keV doublet

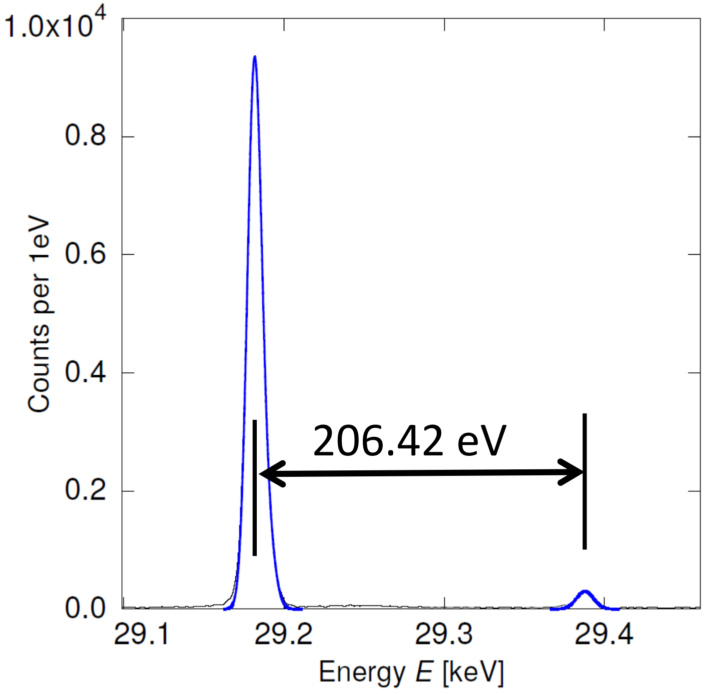

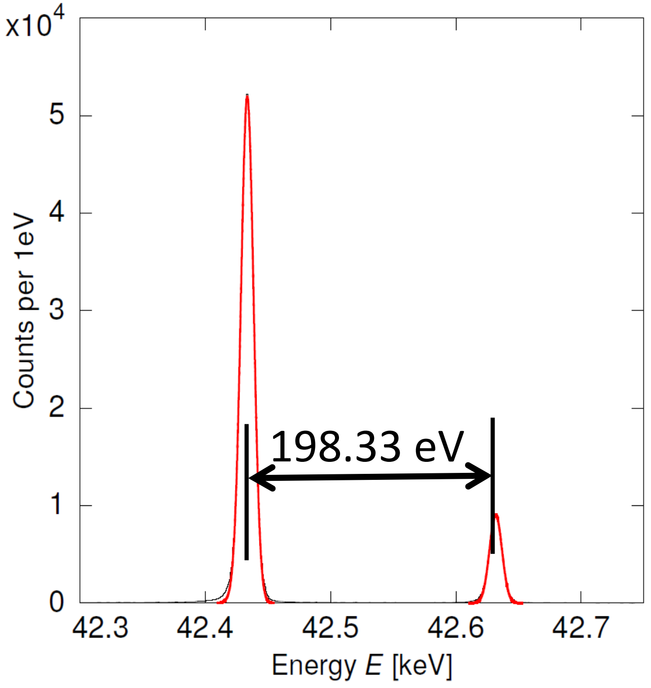

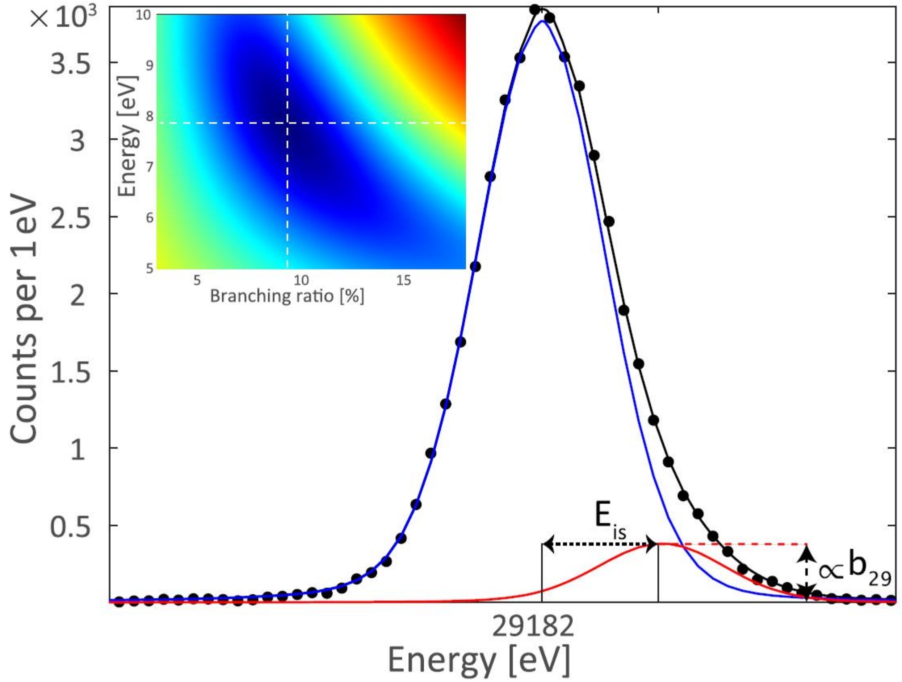

Isomer energy: ΔE_{iso} = 8.10 eV ± 0.17 eV

Isomer energy: E_{iso} = 7.84 eV +/- 0.3 eV

T. Sikorsky et al., *Phys. Rev. Lett.* **125** (2020) 142503

Highly ionized heavy ions

Study of heavy, highly-charged ions allows

high precision QED measurements in extreme E-fields

→ spectroscopy of H-like and He-like Uranium ions

Talk by Nancy Paul tomorrow 10:00

Poster by Louis Duval

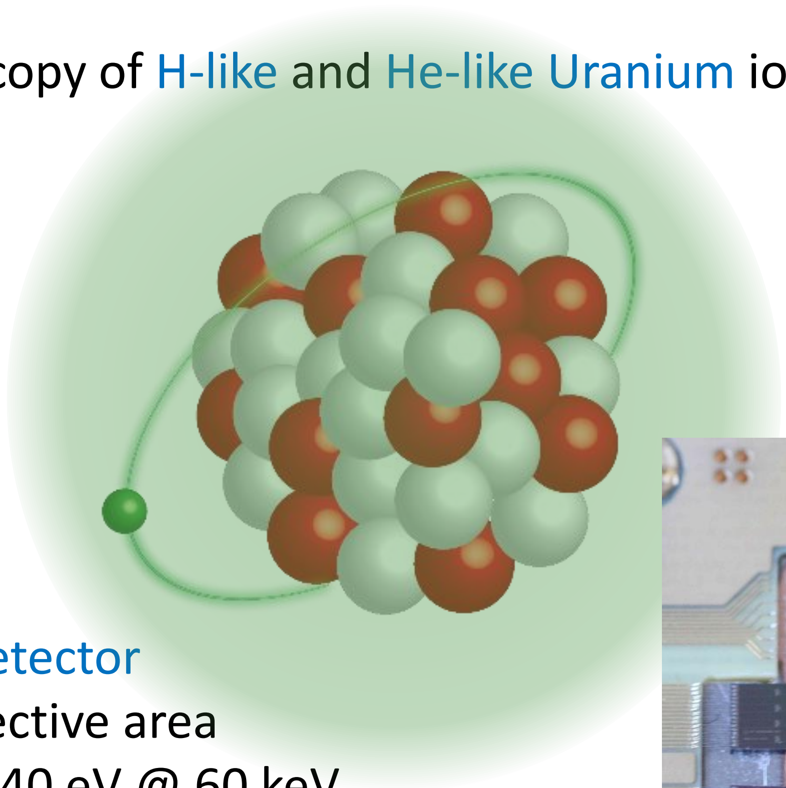

With:

maXs-100 detector

- 1 cm^2 effective area
- ΔE_{FWHM} = 40 eV @ 60 keV
- Non-linearity ~ 0.2 % @ 136 keV
- 300 ns coincidence capability

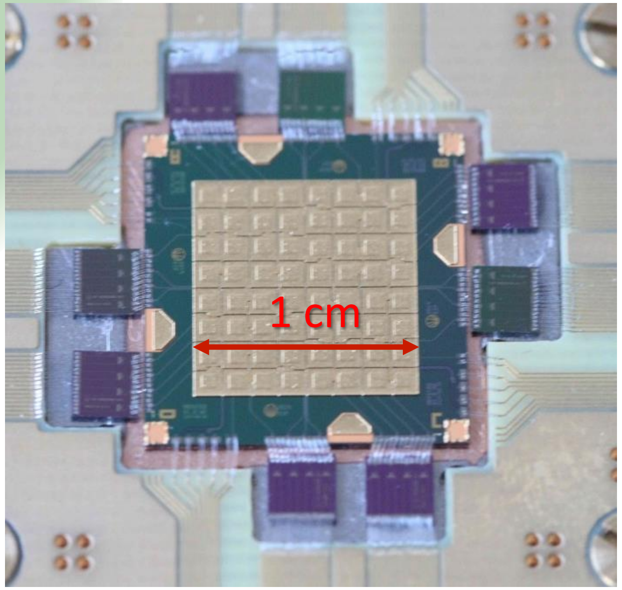

Where:

GSI cryring

Major players:

Andreas Fleischmann, Daniel Hengstler

GSI – Darmstadt: 2 weeks beamtime

LINAC
Accelerate to 11.4 MeV/u

SIS
Accelerate to 400 MeV/u

Stripper foil:
remove all but one electron

ESR
Decelerate to 10 MeV/u

CRYRING
Stored ion beam

sparc
Stored Particles Atomic Physics Research Collaboration

Experimental configuration

Electron cooler

- Superimpose electron and ion beam
- Reduce momentum spread
- $U^{91+} + e^- \rightarrow U^{90+} + \gamma$

2 detector systems

- At 0° and 180° scattering angle
- 13 keV red shift @ 180°
- 15 keV blue shift @ 0°
- intrinsic Doppler shift correction

2x maXs100

- In total 102/128 pixels operated
- Energy resolution
    - 80 eV FWHM @ 122 keV
    - 60 eV FWHM @ 122 keV

Composite calibration source

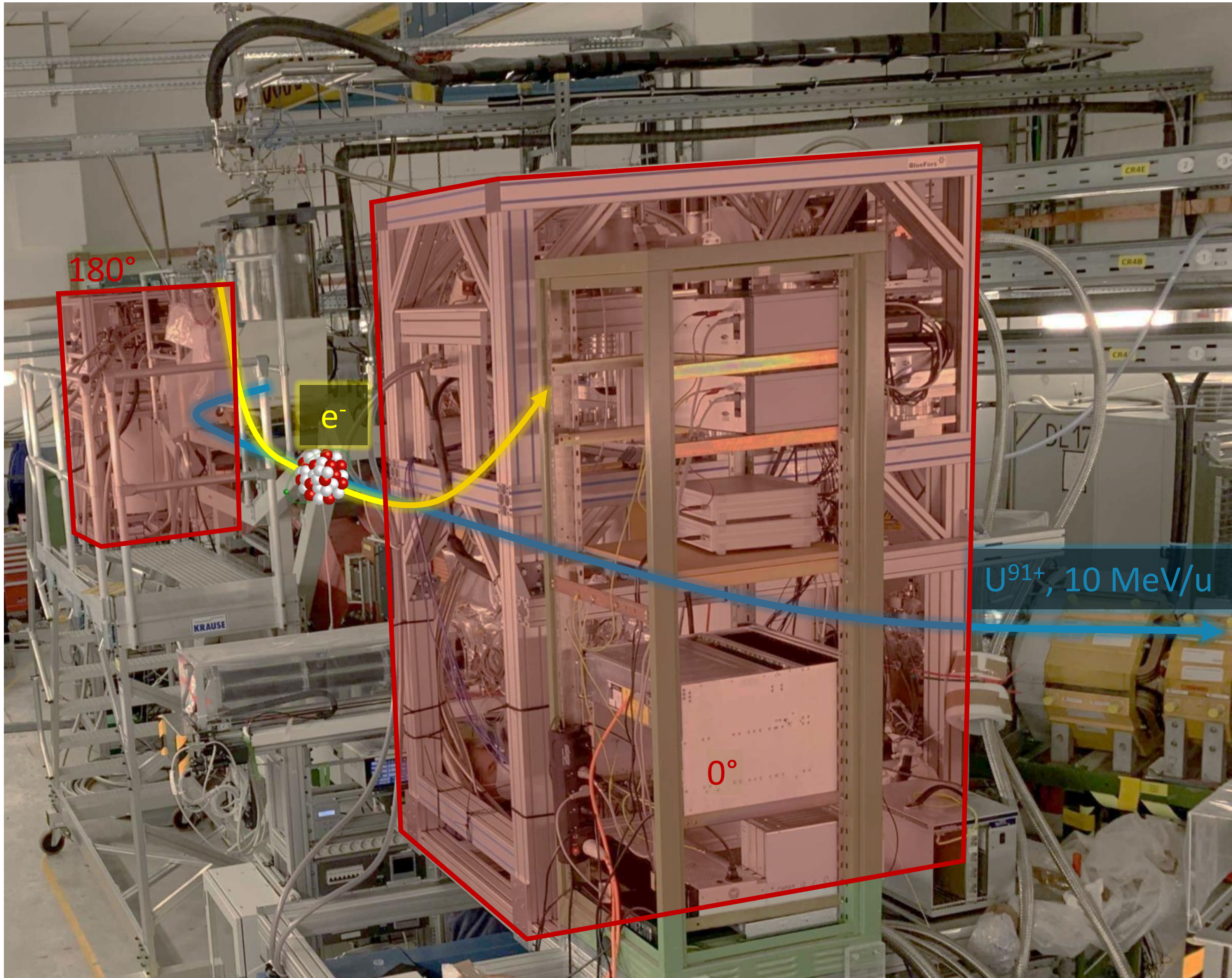

Highly ionized heavy ions – U^{90+}

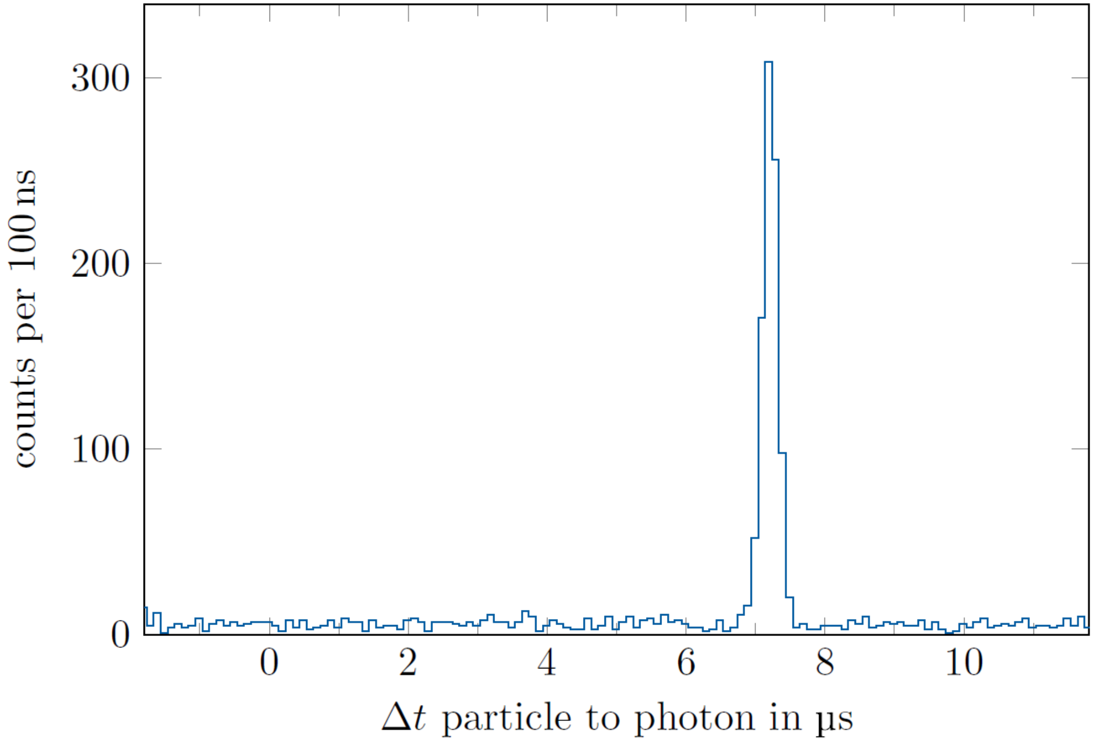

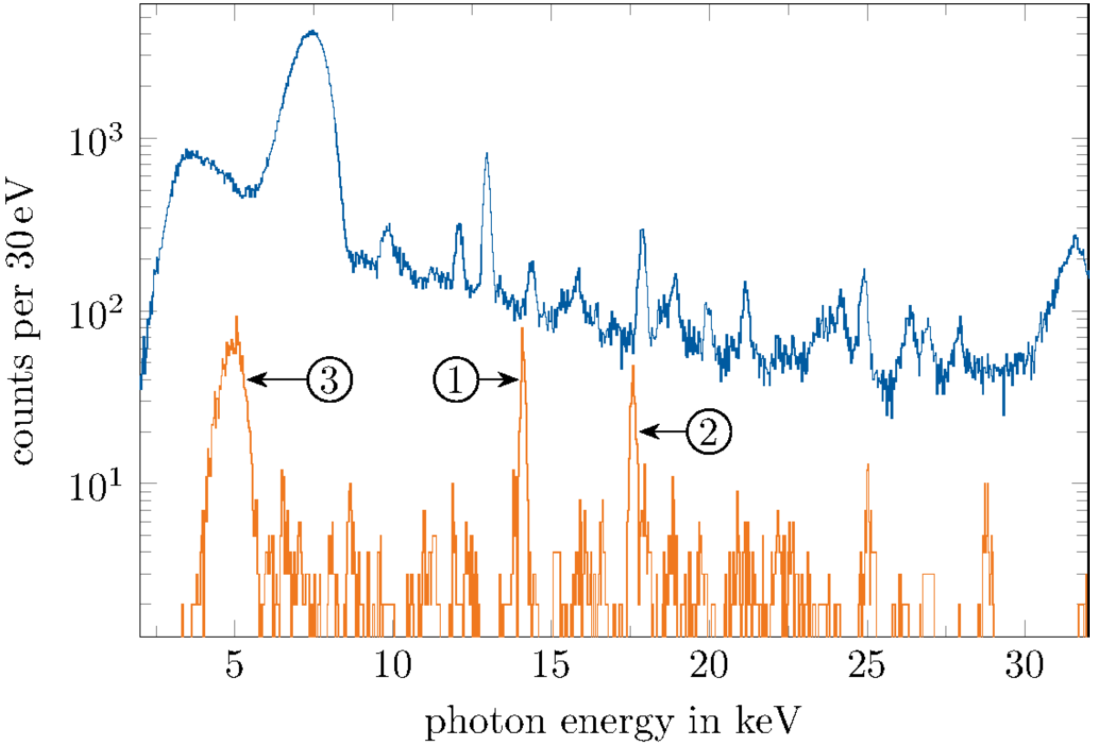

Photons emitted by ions undergoing radiative recombination with the cooler electrons show a fixed time delay wrt the signal due to the ions detection

Transitions can be clearly observed/identified

Analysis still on-going

Ph Pfäfflein *et al* 2022 *Phys. Scr.* **97** 114005

Muonic atoms – QUARTET Collaboration

High energy resolution spectroscopy of muonic atoms for charge radii determination

- Proof of concept experiment with muonic atoms (as Lithium)
  → PSI measurements scheduled October 2023

- Next future goal: study the nuclei in the range $2 < Z < 11$

Talk by Nancy Paul tomorrow 10:00

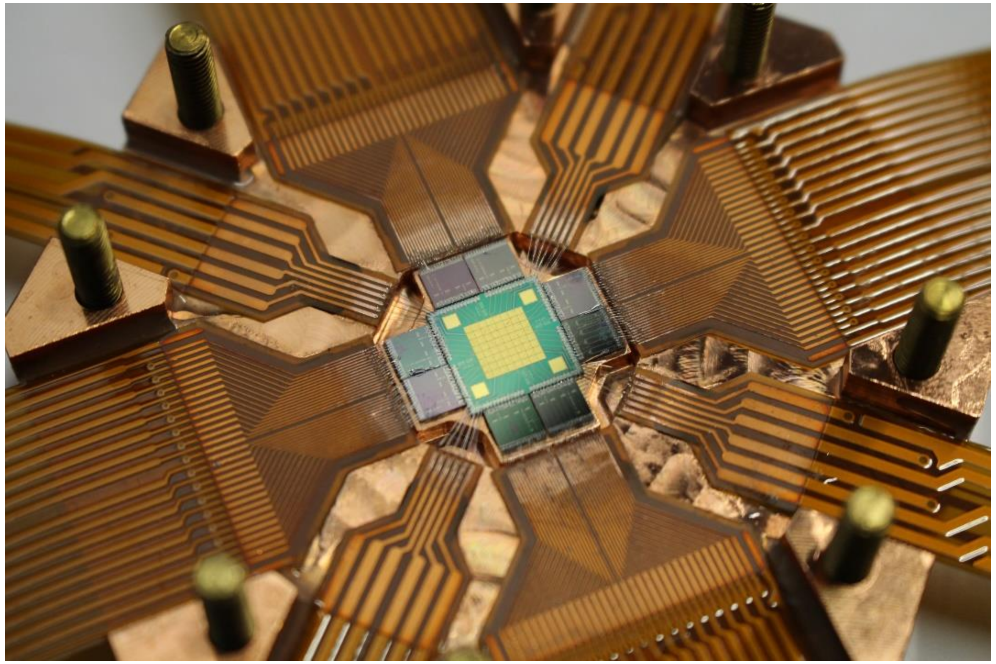

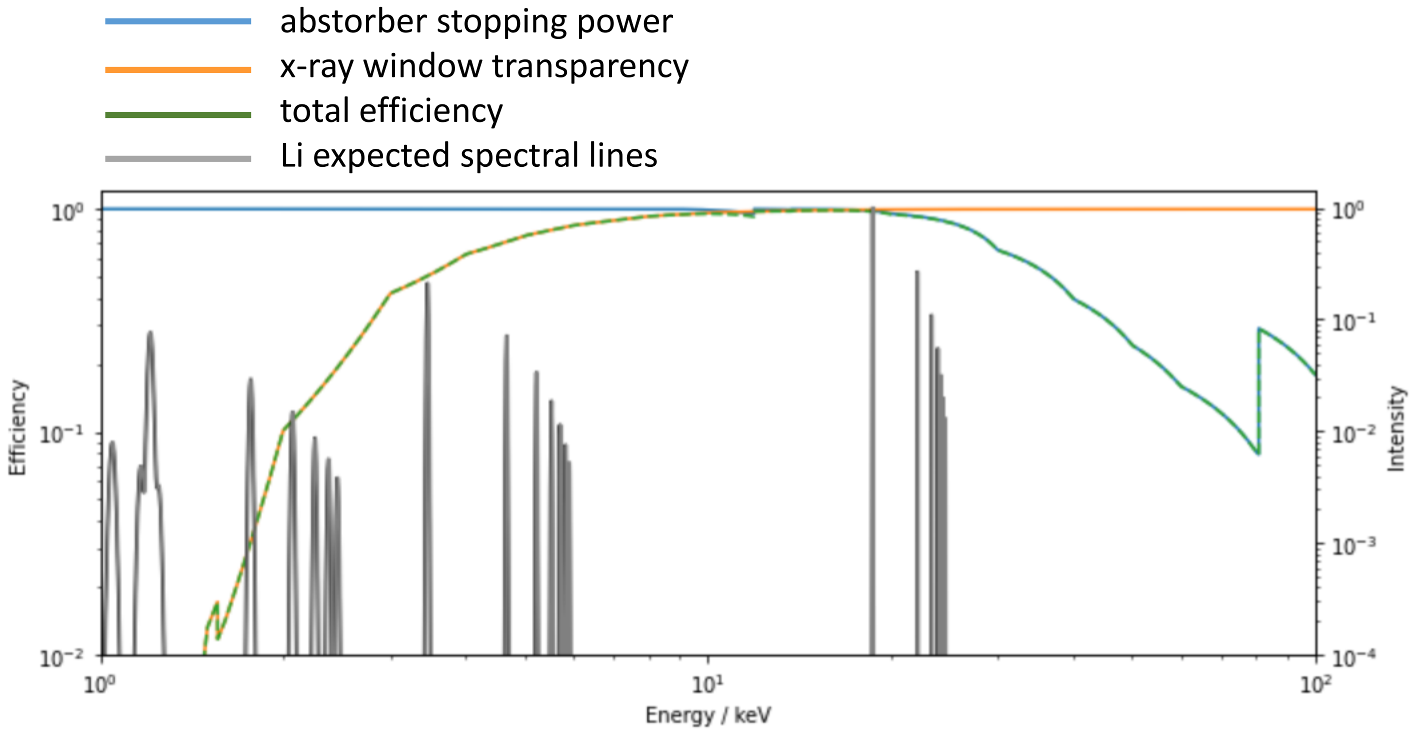

MMCs with electron capture sources

MMC absorbers can be fabricated with 100% stopping power for radiation emitted by an internal source

Ion-implantation to reduce host material effects

Electron capture generates excited atomic stated whose energy can be precisely determined

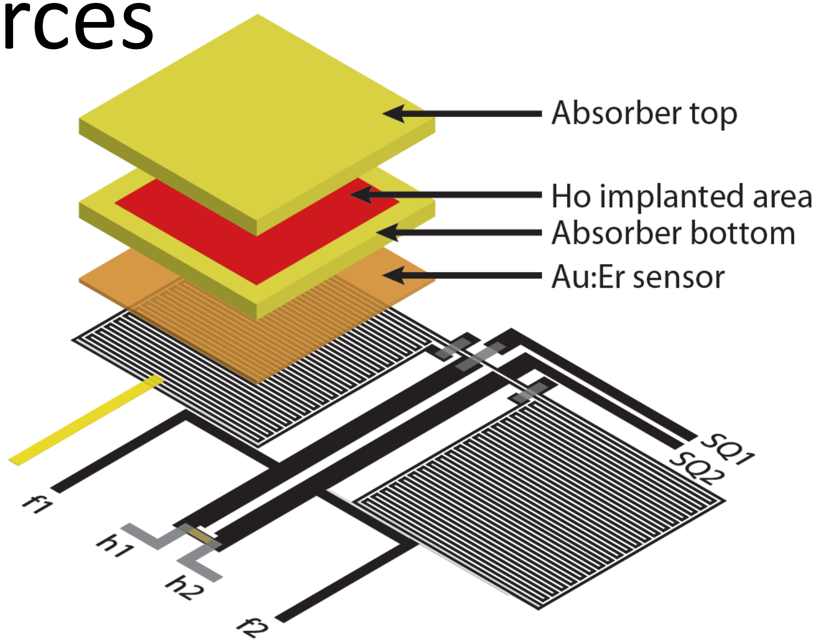

MMCs for the ECHo experiment

ECHo uses large arrays of MMCs with enclosed ^{163}Ho

$$^{163}_{67}\mathrm{Ho} \rightarrow ^{163}_{66}\mathrm{Dy}^* + \nu_e$$

$$^{163}_{66}\mathrm{Dy}^* \rightarrow ^{163}_{66}\mathrm{Dy} + E_C$$

- $\tau_{1/2} \cong$ 4570 years (2*10^{11} atoms for 1 Bq)
- Q_{EC} = $(2.833 \pm 0.030^{stat} \pm 0.015^{syst})$ keV

S. Eliseev et al., *Phys. Rev. Lett.* **115** (2015) 062501

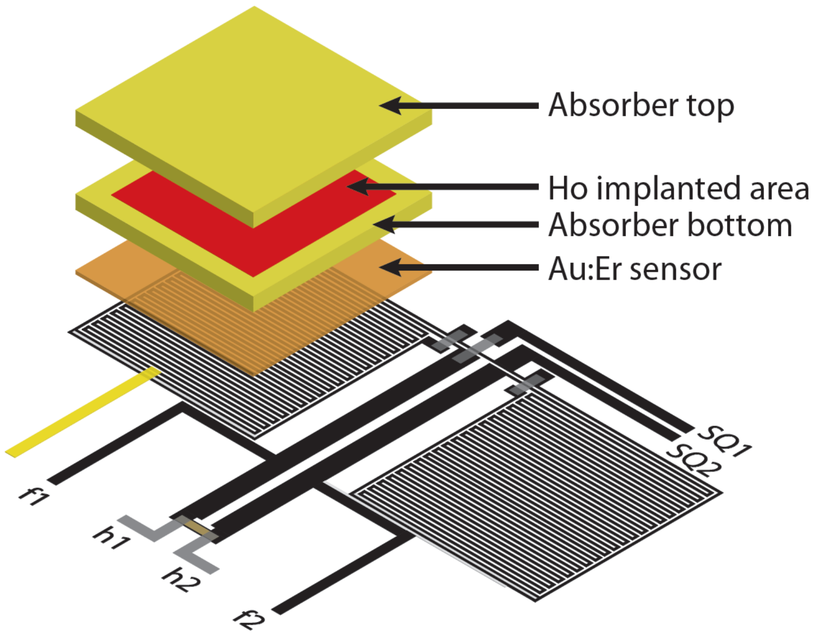

Implantation square:
150 µm x 150 µm

Second absorber:
165 µm x 165 µm

First absorber:
180 µm x 180 µm

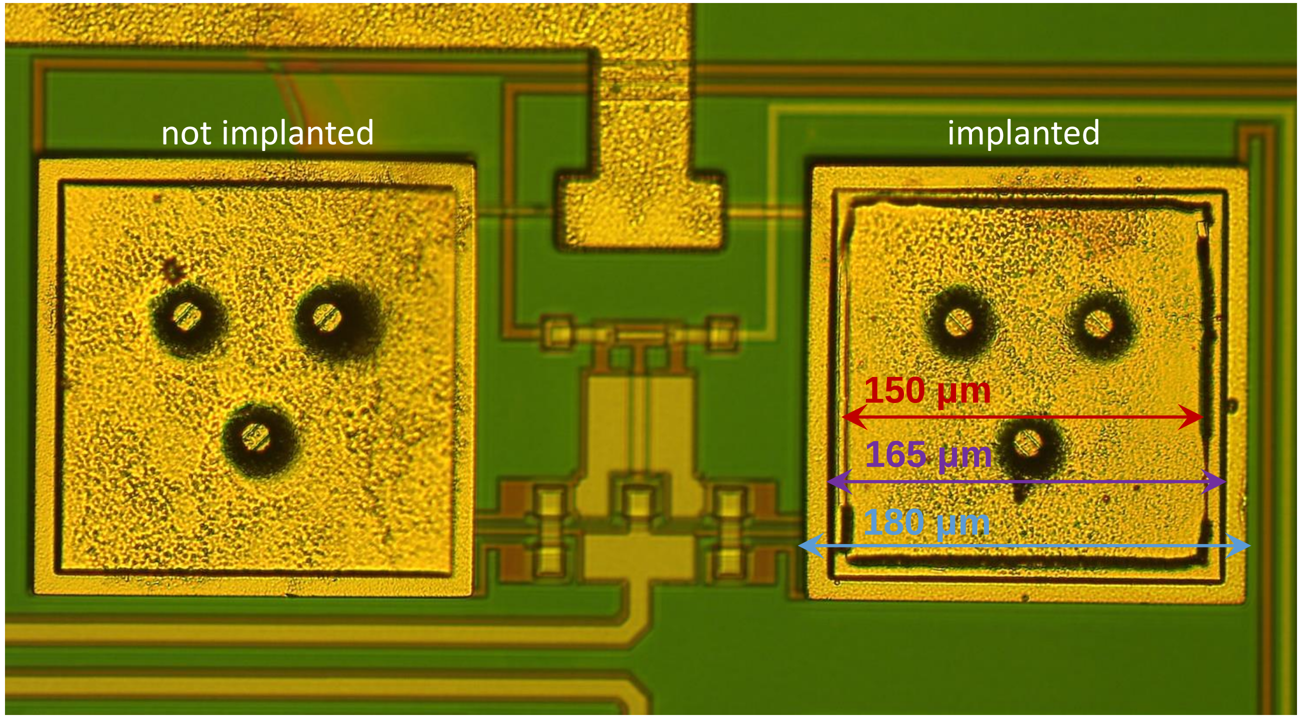

MMCs for the ECHo experiment

ECHo uses large arrays of MMCs with enclosed ^{163}Ho

$$^{163}_{67}\mathrm{Ho} \rightarrow ^{163}_{66}\mathrm{Dy}^{*} + \nu_{\mathrm{e}}$$

$$^{163}_{66}\mathrm{Dy}^{*} \rightarrow ^{163}_{66}\mathrm{Dy} + E_{\mathrm{C}}$$

- $\tau_{1/2}$ ≅ 4570 years (2*10^{11} atoms for 1 Bq)
- Q_{EC} = $(2.833 \pm 0.030^{\mathrm{stat}} \pm 0.015^{\mathrm{syst}})$ keV

S. Eliseev et al., *Phys. Rev. Lett.* **115** (2015) 062501

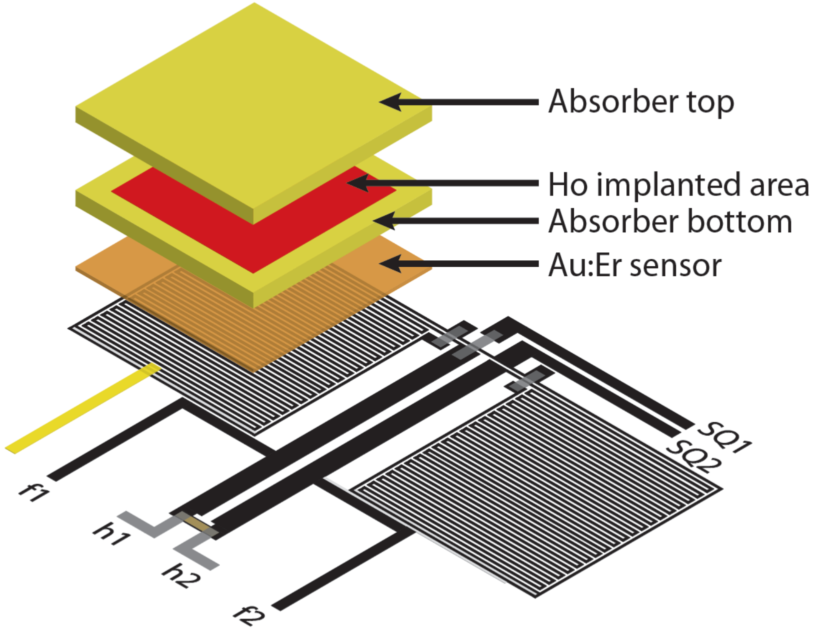

Implantation square:
150 µm x 150 µm

Second absorber:
165 µm x 165 µm

First absorber:
180 µm x 180 µm

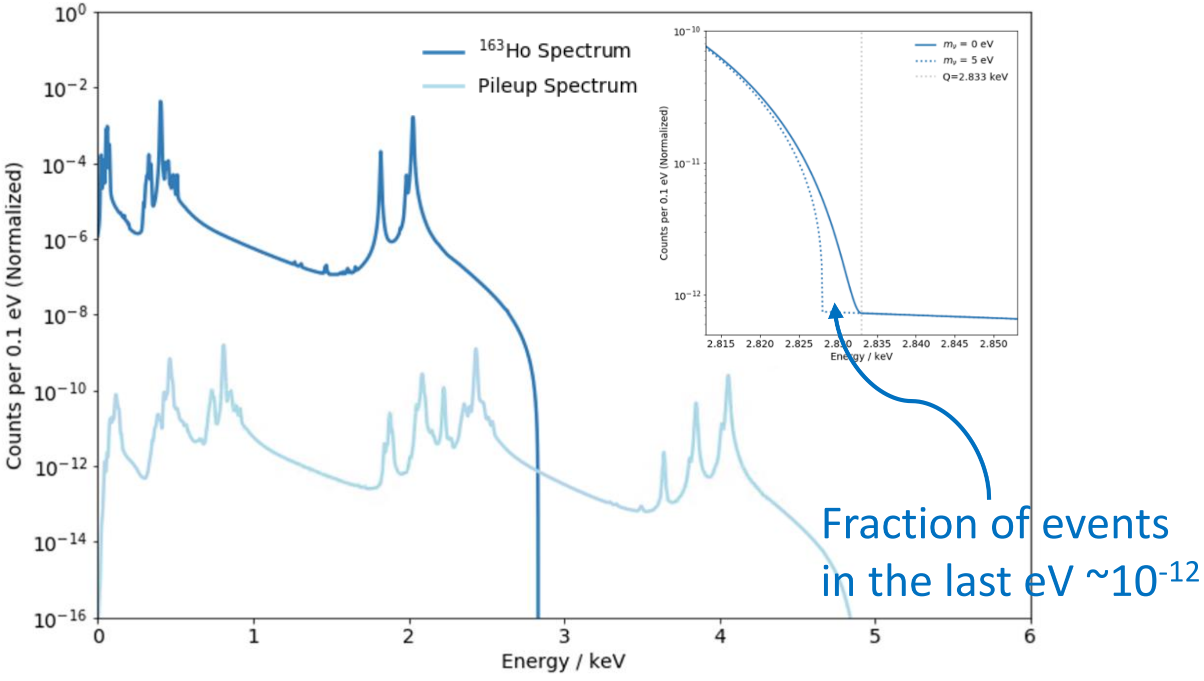

M. Braß and M. W. Haverkort, *New J. Phys.* **22** (2020) 093018

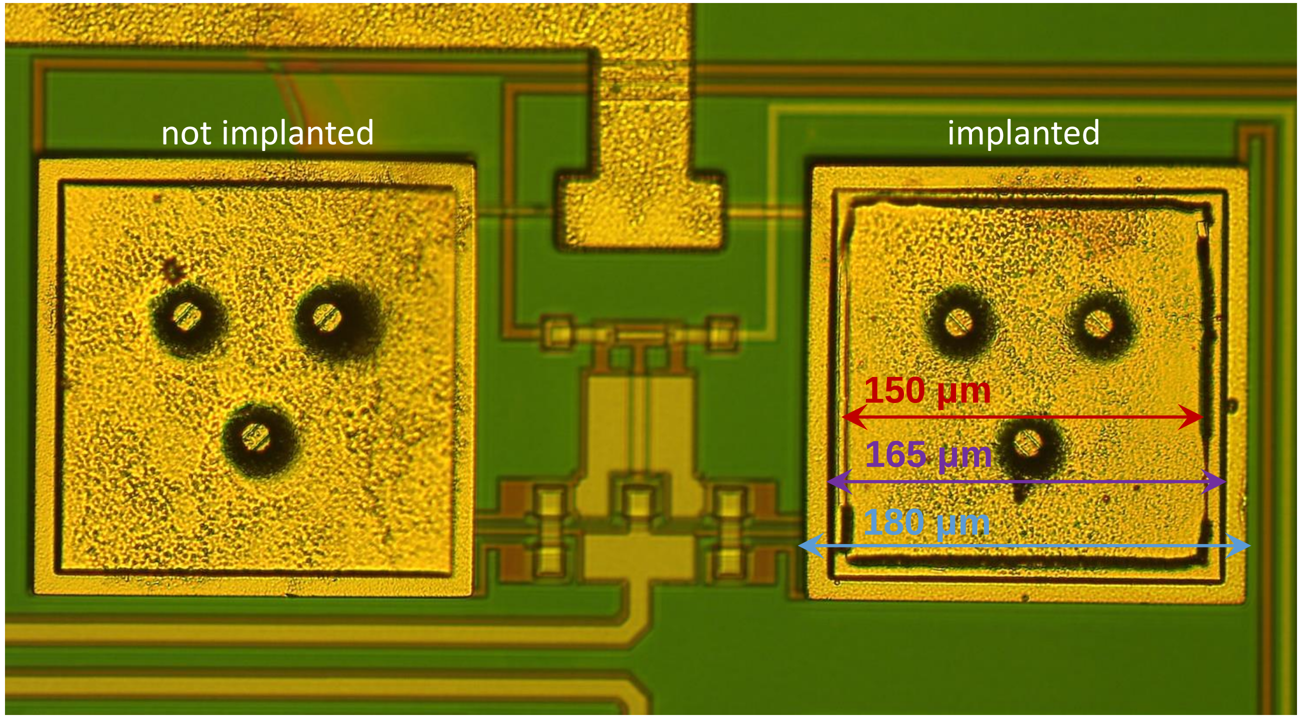

High energy resolution ^{163}Ho spectrum

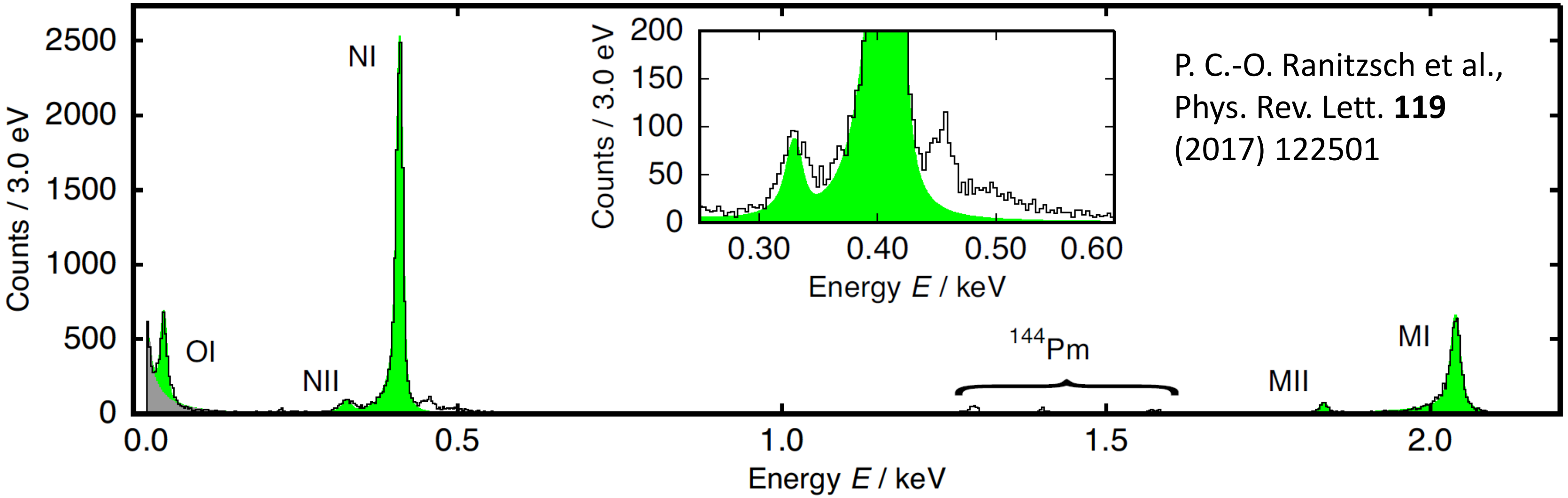

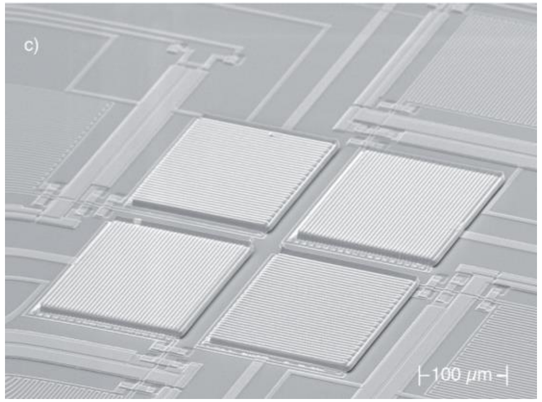

Identification of non-expected structures in the spectrum

High energy resolution ^{163}Ho spectrum

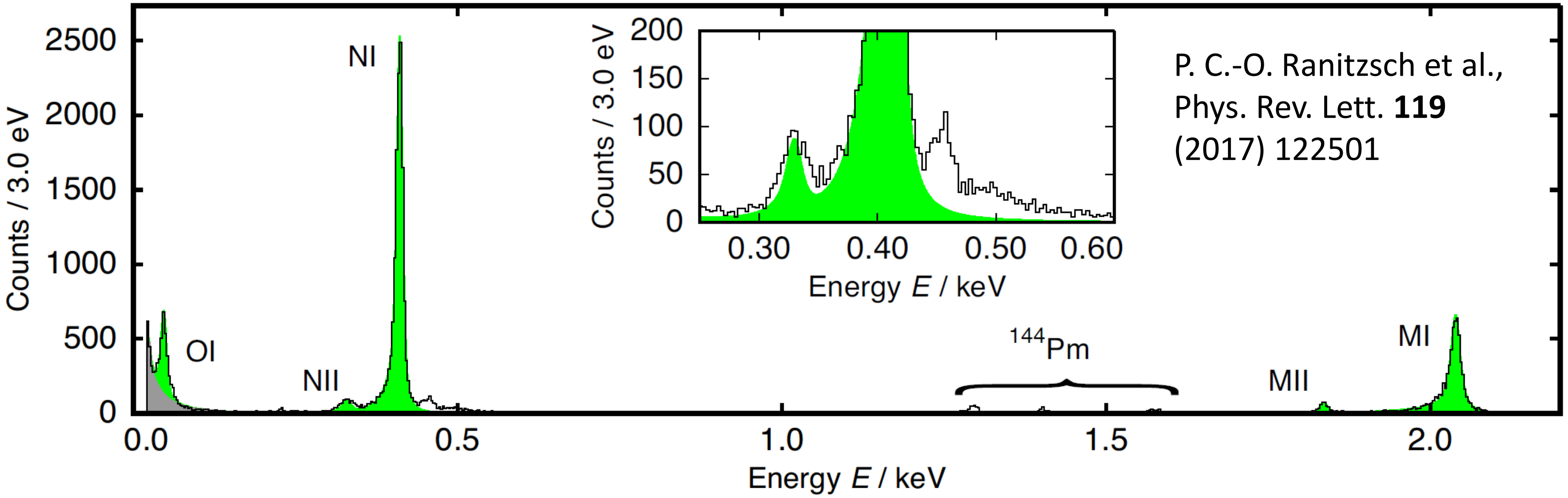

P. C.-O. Ranitzsch et al., Phys. Rev. Lett. **119** (2017) 122501

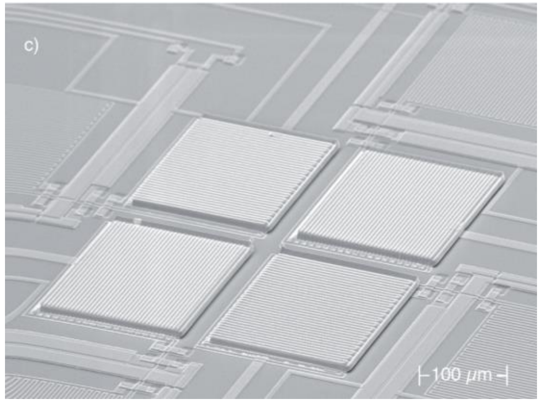

Identification of non-expected structures in the spectrum

- A. Faessler et al.
  J. Phys. G **42** (2015) 015108
- R. G. H. Robertson
  Phys. Rev. C **91**, 035504 (2015)
- A. Faessler et al.
  Phys. Rev. C **91**, 064302 (2015)
- A. Faessler and F. Simkovic
  Phys. Rev. C **91**, 045505 (2015)
- A. De Rujula and M. Lusignoli
  JHEP 05 (2016) 015, arXiv:1601.04990v1
- A. Faessler et al.
  Phys. Rev. C **95**, (2017) 045502

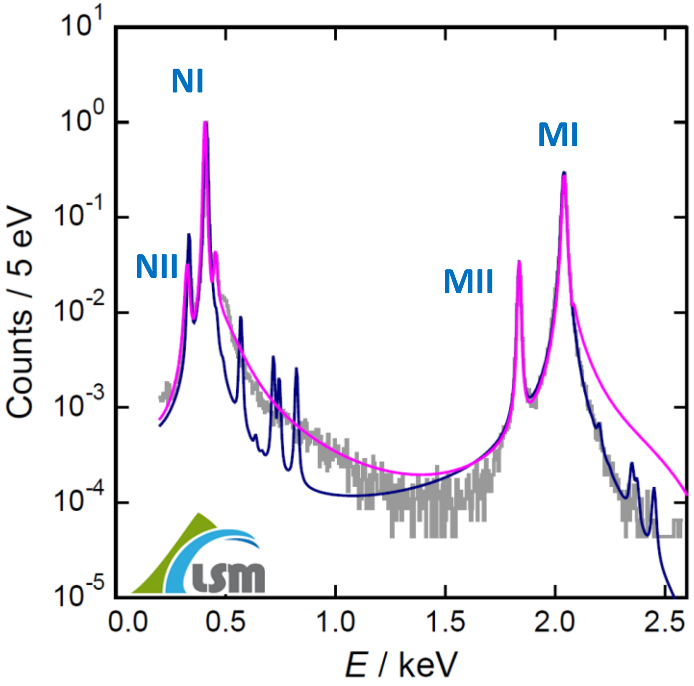

High energy resolution ^{163}Ho spectrum

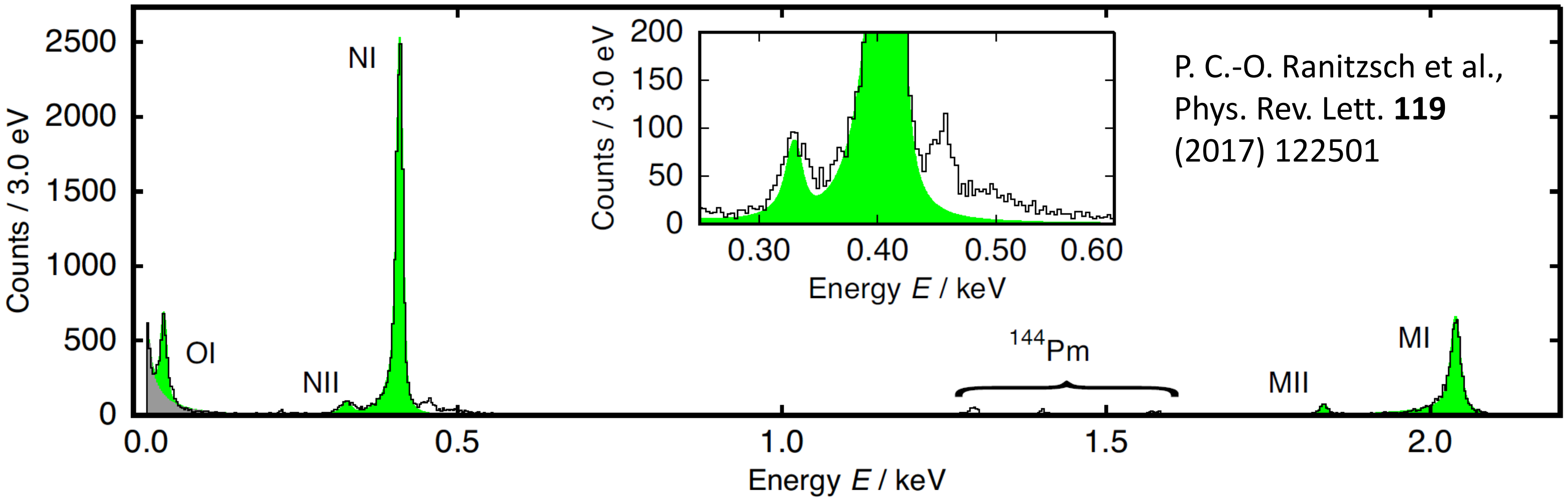

P. C.-O. Ranitzsch et al., Phys. Rev. Lett. **119** (2017) 122501

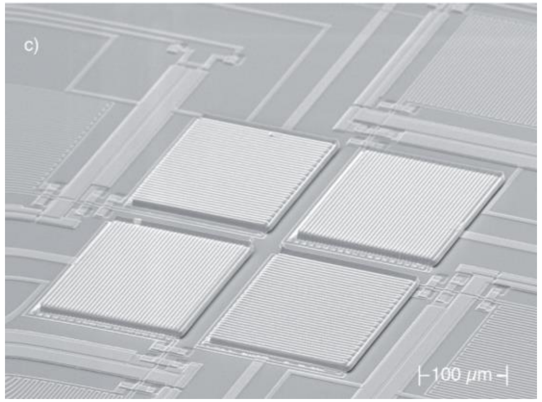

Identification of non-expected structures in the spectrum

New approach

Ab initio calculation of the ^{163}Ho electron capture spectrum

Restricted to bound-states only, i.e. the spectrum is given by a finite number of resonances

M. Braß et al., *Phys. Rev. C* **97** (2018) 054620

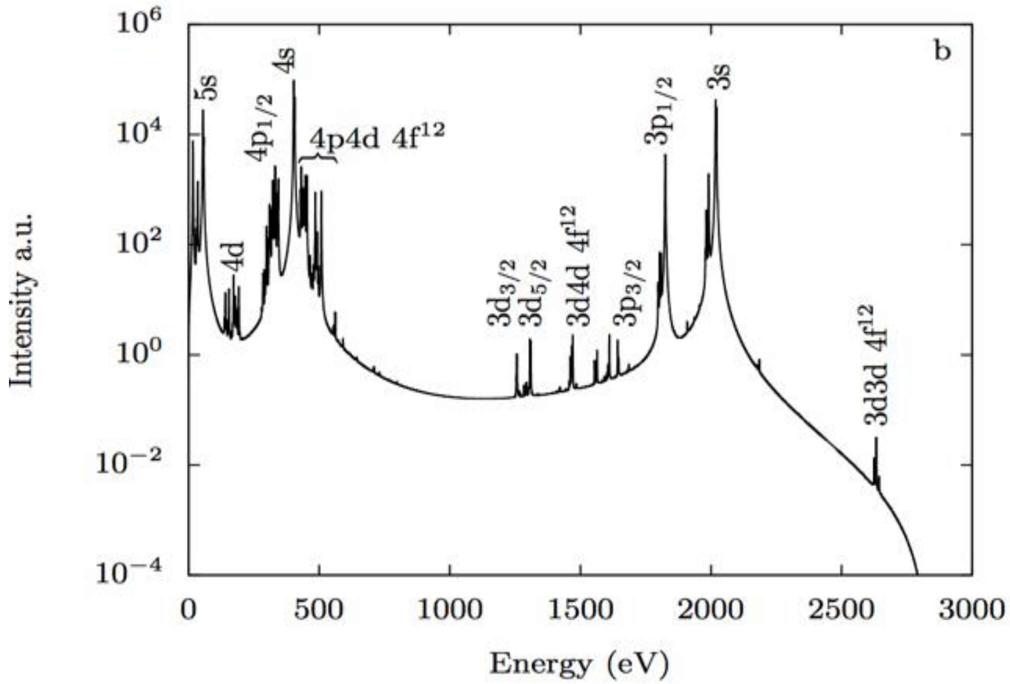

High energy resolution ^{163}Ho spectrum

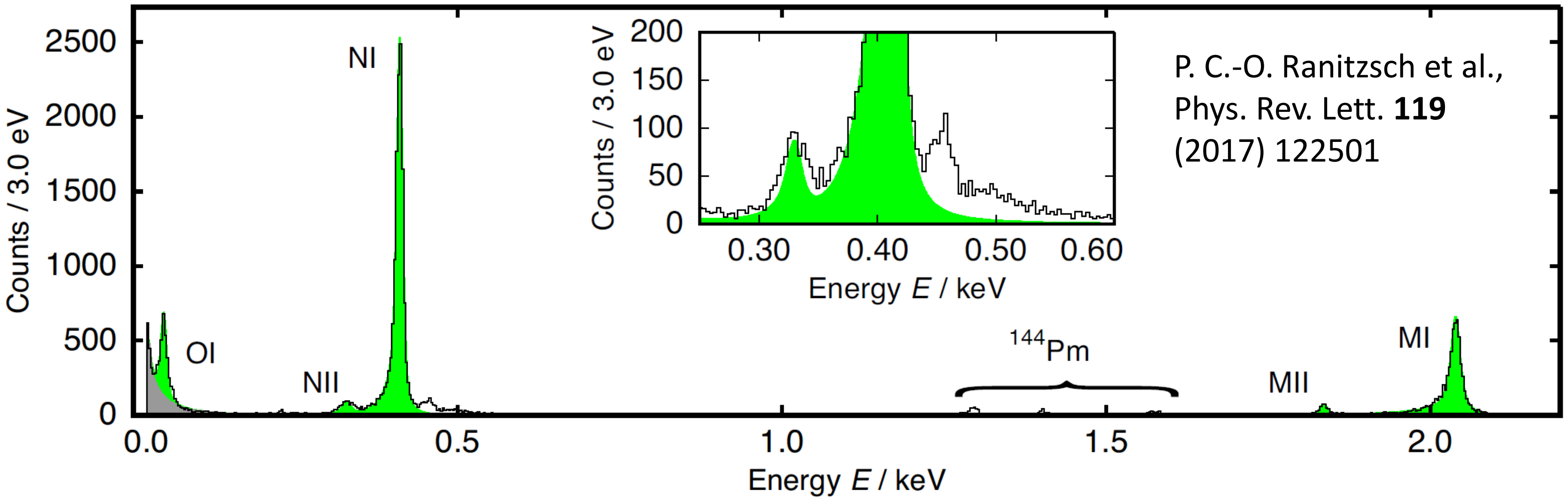

P. C.-O. Ranitzsch et al., Phys. Rev. Lett. **119** (2017) 122501

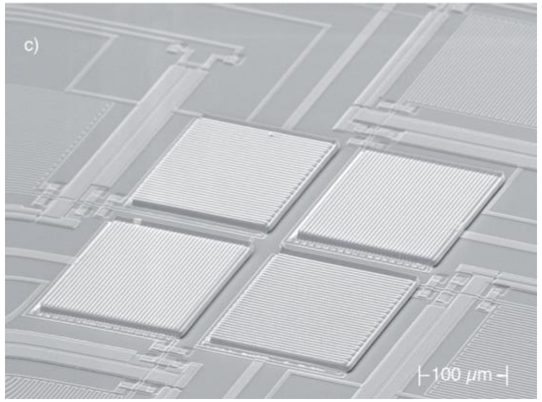

Identification of non-expected structures in the spectrum

New approach

Ab initio calculation of the ^{163}Ho electron capture spectrum

Restricted to bound-states only, i.e. the spectrum is given by a finite number of resonances

M. Braß et al., *Phys. Rev. C* **97** (2018) 054620

Including states with multiple correlated holes in local atomic orbitals interacting with unbound Auger-Meitner electrons

M. Braß and M. W. Haverkort, *New J. Phys.* **22** (2020) 093018

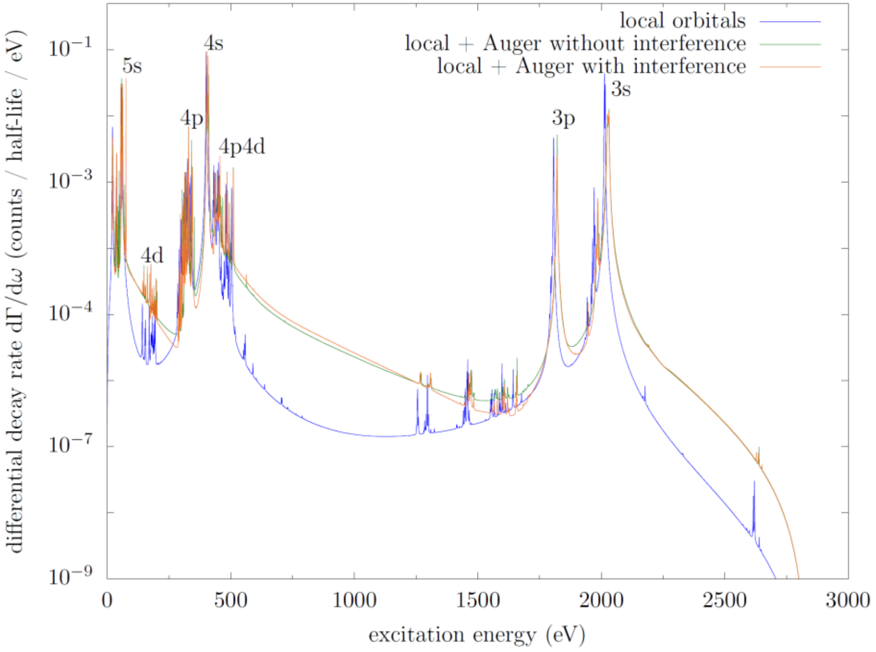

High energy resolution ^{163}Ho spectrum

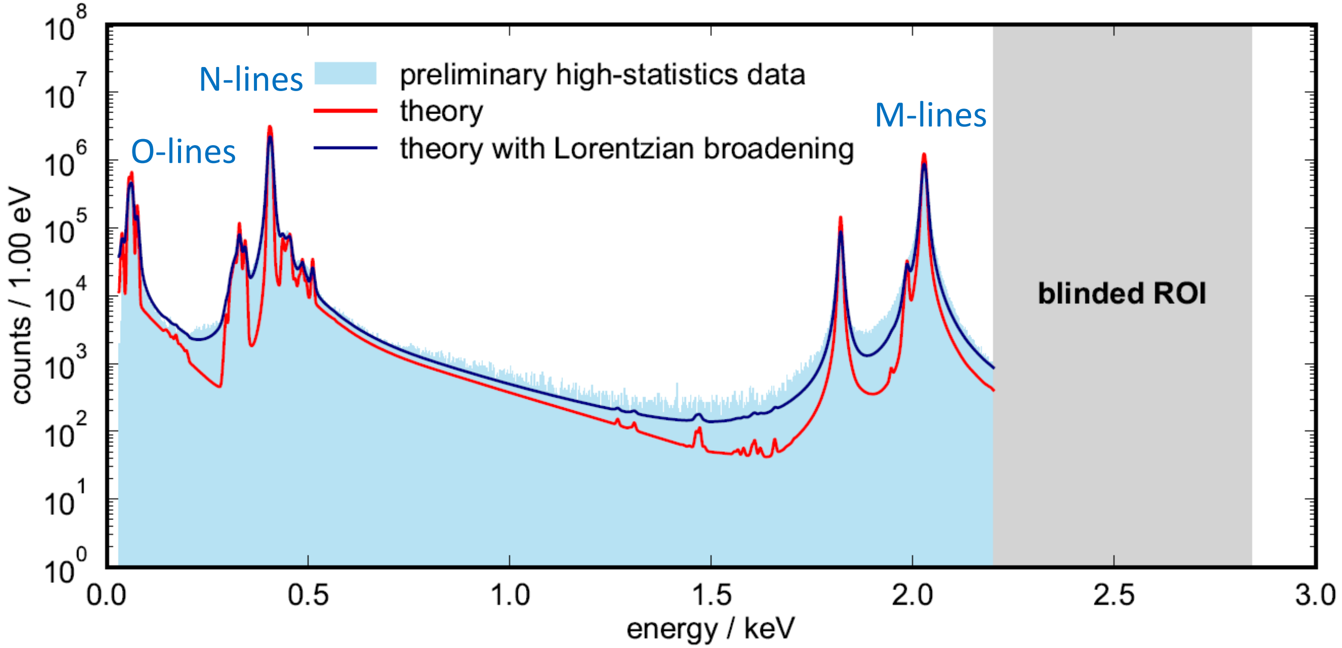

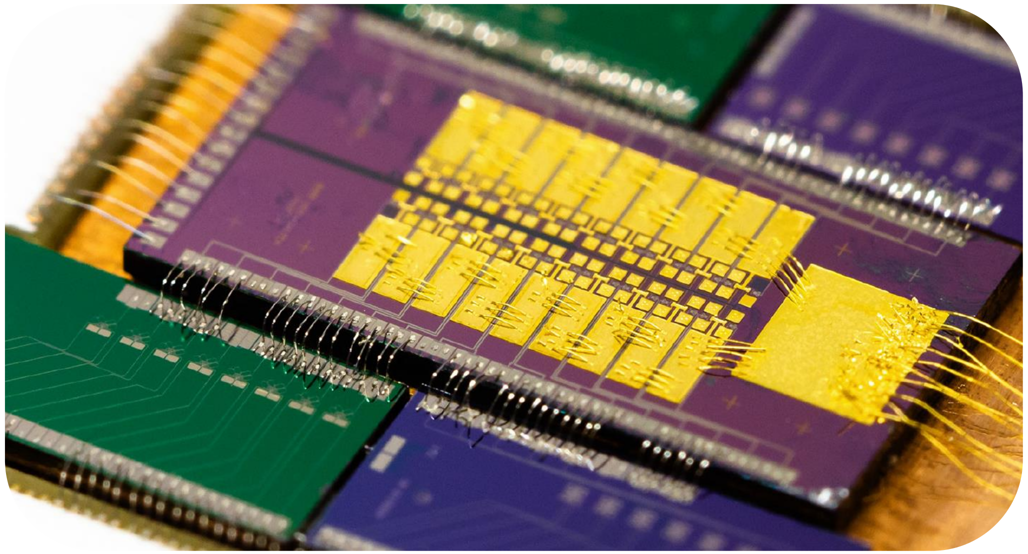

Data corresponding to 6×10^7 events acquired with detectors having ^{163}Ho in Ag

- Only data passing quality checks
- Energy scale defined in a new calibration measurement

New theory describes well the complex structure of line multiplets but tails are still not perfect

- more work is on extending the theoretical description and EC spectra measurements

M. Braß et al., *Phys. Rev. C* **97** (2018) 054620,
M. Braß M. W. Haverkort, *New J. Phys.* **22** (2020) 093018

Conclusions

Metallic magnetic calorimeters

- are versatile low temperature detectors
- high resolution for all kinds of particles
- wide range of energies
- impressive resolving power

High resolution spectra with external and internal sources

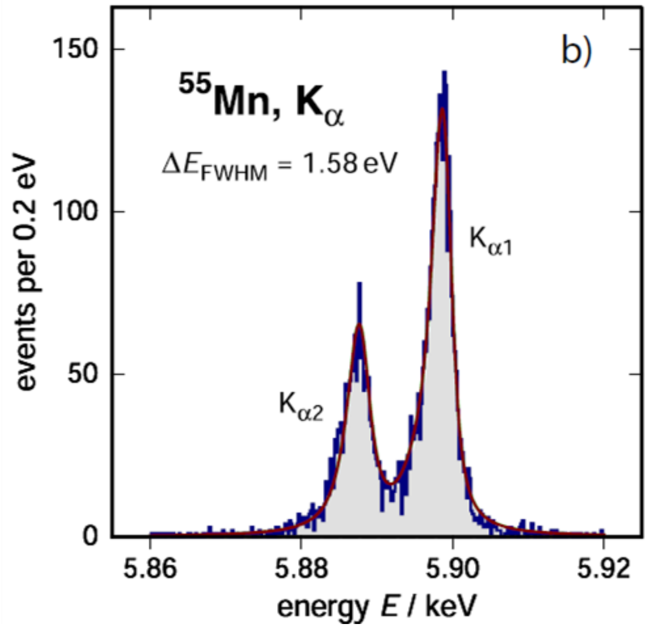

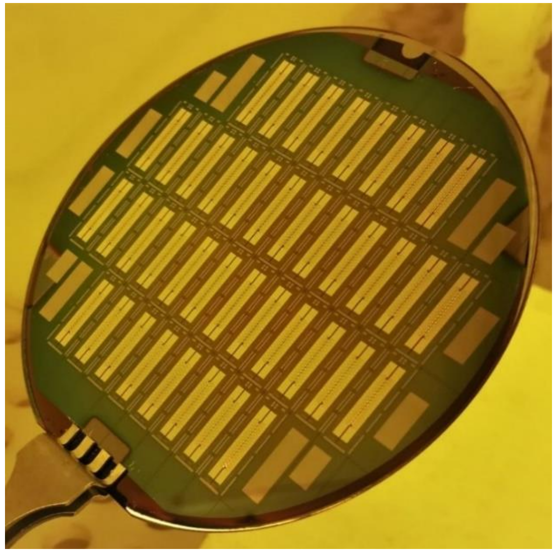

Thank you for the attention!